A.E.E.T.-254

NDS LIBRARY COPY

A.E.E.T.-254

सत्यमेव जयते

GOVERNMENT OF INDIA
ATOMIC ENERGY COMMISSION

VAN DE GRAAFF LABORATORY PROGRESS REPORT

Compiled by
T. P. David
Nuclear Physics Division

ATOMIC ENERGY ESTABLISHMENT TROMBAY
BOMBAY, INDIA
1966

A.E.E.T-254

GOVERNMENT OF INDIA
ATOMIC ENERGY COMMISSION

A.E.E.T.-254

VAN DE GRAAFF LABORATORY
PROGRESS REPORT

Compiled by

T.P.David
Nuclear Physics Division

ATOMIC ENERGY ESTABLISHMENT TROMBAY
BOMBAY, INDIA
1966

CONTENTS

****

INTRODUCTION

This report covers the operation and utilization of the 5.5 MeV Van de Graaff Accelerator in the year 1965, the fourth year of operation of the accelerator. Throughout this period the machine has been operating on round the clock basis. The communication receiver on the control console used for measuring the NMR frequency has been replaced with a precision Hewlett Packard frequency counter. This has enabled accurate determination of the beam energy. It is now possible to vary the energy in very small steps and to reproduce energy settings with a very high degree of accuracy as is required for the precision measurement of threshold and resonance energies. A tape punch unit has been added to the TMC 400 channel analyser. The punched tape can be fed directly into the computer, considerably reducing the time needed for analysing the data obtained from the 400 channel analyser.

The research programme with the accelerator has been aimed at a study of nuclear reactions and nuclear structure utilizing charged particle reactions. The nuclear reactions studied include proton and alpha induced reactions for light and medium weight nuclei involving single level resonance theory, fluctuation theory and stripping theory. Angular correlation experiments for deuteron induced such as $(d, p\gamma)$ reactions, aimed at studying low lying levels of nuclei, have also been undertaken.

ACCELERATOR

The Accelerator operation during this period can be analysed as given under:

1.	Total time available from 1st January to 31st December 1965	..	8760 Hours
2.	Observed holiday hours during the year	..	24 Hours
3.	Time for fortnightly routine maintenance work	..	624 Hours
4.	Other maintenance work	..	360 Hours
5.	Shut down due to failure of power and water supplies	..	336 Hours
6.	Time used for Gas system modifications and ion source development	..	384 Hours
7.	Total time of Accelerator run	..	5788 Hours
8.	Time lost due to breakdowns	..	1244*Hours
9.	Machine time used for development work	..	400 Hours
10.	Time used for research experiment	..	4624 Hours
11.	Time lost in machine conditioning and auxiliary repairs	..	463 Hours
12.	Time lost due to malfunction of experimental facilities	..	301 Hours

---

* In this, 744 hours have been spent for transfer of insulating gas and accelerator tank roughing

I. Modification to the Accelerator:

1. A new gas manifold designed to accommodate 4 gas bottles (H_2, D_2, ^3He and ^4He) and their gas leaks has been fabricated and installed in the top terminal of the accelerator.

2. The gas feed arrangement has been replaced with a new compact unit. This unit which selects one of the four gases and lights the gas-indicating lamps, consists of a battery of eight microswitches operated by a cam shaft. The pulley attached to the shaft is cord driven by the base plate selsyn motor.

3. The terminal meters have been replaced with edgewise meters assembled in an aluminium box. An additional meter has been provided and wired to read the probe voltage.

4. The original clamp mounting of the dial gauges on the control slit made it extremely difficult to reproduce accurately the setting of the slits. This difficulty has been removed by mounting the dial gauges directly on the moving slit assembly.

5. The tube extension isolation valve was developing through leaks frequently. This has been replaced with a 4" gate valve with the necessary flanges and is found to work satisfactorily.

6. The Hewlett Packard frequency counter has been installed replacing the communication receiver on the control console for measuring the NMR frequency. Energy variation in fine steps and accurate reproduction of energy settings are now made possible.

7. The beam deflector assembly designed and fabricated in the Van de Graaff laboratory[1)] has been installed in one of the 30° side ports of the switching magnet.

This is of considerable use for steering the beam on to the target when fine collimation is required. Two similar beam deflector are under fabrication for installation in the other beam ports.

Reference:

(1) T.P.David, Van de Graaff Progress Report, A.E.E.T.-214 (1965)

II. Accelerator breakdowns and repairs:

There were two long periods of accelerator breakdowns; one for about 2 weeks (March 4 to 17th) and another for about 3 weeks (from August 12th to 31st). During both these periods a number of defects developed one after another which include vacuum leaks into the tubes, failure of electrical insulation and breakdown of electron components in the control circuits.

Some of the major breakdowns and remedies carried out durin the period under review are listed below:

1. Visible cracks developed on four glass sections of the accelerating tube. Since these did not cause any gas leak into the tube when the tank was pressurised, the damaged sections have been electrically shorted.

2. Tube pressure was found to rise when the tank was being pressurised. It was found that the tube pressure rose when the tank pressure increased above 100 p.s.i. and fell again when the tank pres increased above 180 - 185 p.s.i. The defect was traced to a minor l in the bellow seal of the hoke valve in the gas feed line.

3. Accelerator potential was found increasing when focus voltage was raised. This was caused by a gas leak heater lead touching the inside of the dome and was rectified.

4. The perspex mounting of the corona point assembly was found cracked due to sparking. A new mounting was made and installed.

5. Thyrite protective resistors in the belt charge circuit developed sparking to the base plate. The resistors were mounted on the base plate providing sufficient clearance to ground.

6. The cable connecting belt charge supply unit to the high voltage bushing on the base plate developed leakage. The cable was replaced.

7. Terminal pulley alternator winding developed a ground short. The shorted coil was rewound.

8. Shorting relays in the high voltage unit of the belt charge supply burnt out and were renewed.

9. 80 KV insulation bushings on the terminal developed leakage, loading the alternator when focus voltage was increased. New perspex bushings were fabricated and installed.

10. NMR oscillator frequency was found drifting after its being 'on' for a couple of hours. The defect was traced to a faulty potentiometer in the filament voltage stabilizer circuit.

III. Development Projects:

1. Five port beam switching magnet[1)] - T.P.David and N. Sarma - The Aluminium vacuum chamber for the magnet is under fabrication in the Nuclear Physics Division workshop. The construction of the magnet yoke could not be taken up due to the delay in the delivery of the

Tata 'A' grade steel. The magnet coil has been redesigned and is to be made from electrical grade Aluminium tubing of square section 12.7 mm and thickness 1.65 mm. Insulation between the magnet coil layers will be provided by anodising the aluminium tubing. The cooling water will be circulated through these tubes forming the magnet coil thus giving maximum cooling efficiency. The separate cooling chambers are thus dispensed with. The power requirement is estimated to be approximately 125 Amps at 20 volts.

2. Ion source assembly - R.P. Kulkarni - Ion sources give a useful service of 300 - 400 hours after which the efficiency falls rapidly. Since the accelerator is working on round the clock basis, these are to be renewed approximately every two weeks of accelerator operation. An attempt has been made to fabricate ion sources locally. A prototype has been built and is undergoing tests. A laboratory system for testing the yield and stability of these sources have been built and assembled. This includes the accelerating column, focusing system and the necessary R.F. oscillator and power supplies. Meanwhile, a method has been developed in the laboratory for reprocessing the otherwise unserviceable ion sources. Such processed ion sources are in use with the accelerator since November 1965. The performance has been very satisfactory, some giving efficient service upto 550 hours.

3. Electromagnetic quadrupole focusing lens[1] - M. Bhatia, N. Thampi and T.P. David - The quadrupole lens assembly installed in the centre port of the switching magnet has given satisfactory service throughout

the year. Two more quadrupole lenses of similar design are under fabrication for installation in the other beam ports. The aperture of the lenses has been increased to 2.54 cms in order to have a wider beam admittance angle.

4. Probe for NMR measurements - P.R.Sunder Rao - A proton resonance probe for use with the NMR oscillator and indicator unit has been constructed. The sample is enclosed in a perspex cylindrical holder as shown in Fig. 1. The R.F. coil has 6 turns of .036" diameter enamel wire and 10 turns of 0.022" diameter enamel wire is used as the modulation coil wound at right angle to the former. Various materials that have been tried as samples are: Liquid paraffin, distilled water, soft rubber, H_2 gas, $FeCl_2$, $FeCl_3$, hydrogenated vegetable oil, coconut oil and transformer oil. Of these the coconut oil is found to give the best result. The shape of the resonance pip obtained at a frequency of 20,000.13 kc/s with a full sweep field modulation of $\sim$ 9 gauss at 50 c/s is given in Fig. 2. An attempt was made to locate lithium resonance by using lithium nitrate and lithium chloride as samples but no indentifiable resonance absorption pip was obtained. Further work is being done to improve the performance of the probe.

5. He^{++} Ion source for Van de Graaff Accelerator[1)] - T.P.David and K.B. Nambiar - Work was done on the system for optimising the yield and focusing conditions. Higher focusing voltage could not be applied due to internal sparking. This was primarily due to inadequate

pumping speed of the vacuum system as also due to insufficient insulation of the glass to metal seal used for focus supply connection. A new vacuum system has been assembled using a 6" oil diffusion pump. The glass to metal seal has been modified to provide for sufficient insulation. The system is undergoing further tests.

6. <u>Transistorised regulated power supply</u> - H.A.P. Kamath - A variable current power supply has been constructed using transistors and silicon diodes. The circuit diagram is given in Fig. 3. The load current is continuously variable from 150 to 800 mA at 40 V. by adjusting the potentiometer P. The setting of this potentiometer determines the base current of Tr_1 balancing against the zener voltage of 6.2 volts at the emitter. This controls Tr_2 wired as an emitter follower which in turn provide the base current for the Darlington pair (Tr_3 and Tr_4) acting as the series element for load stabilization. For a 10% mains voltage fluctuation, the output voltage fluctuation is measured to be ~.5% . The supply is for use with the electromagnetic quadrupole focusing lenses installed in the accelerator beam tube extension.

Reference:

1) T.P. David, Van de Graaff Progress Report, A.E.E.T.-214 (1965).

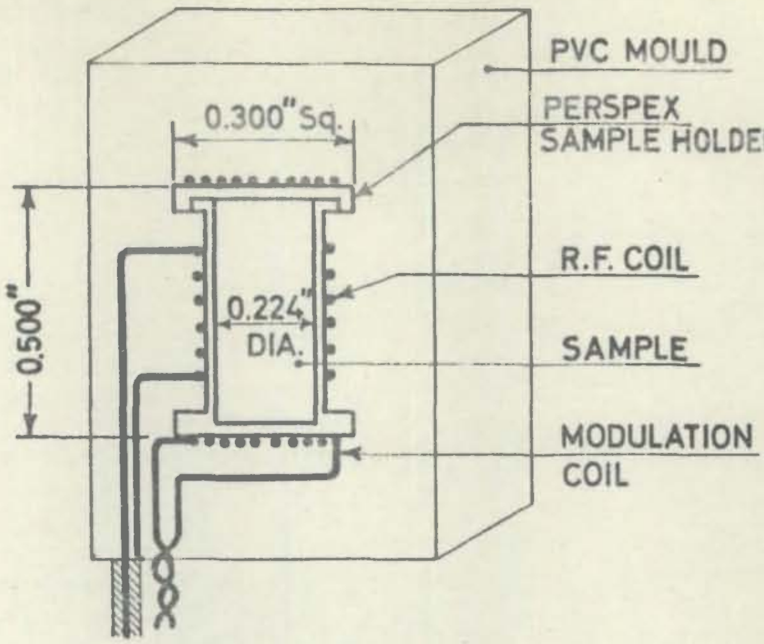

FIG. 1. PROBE

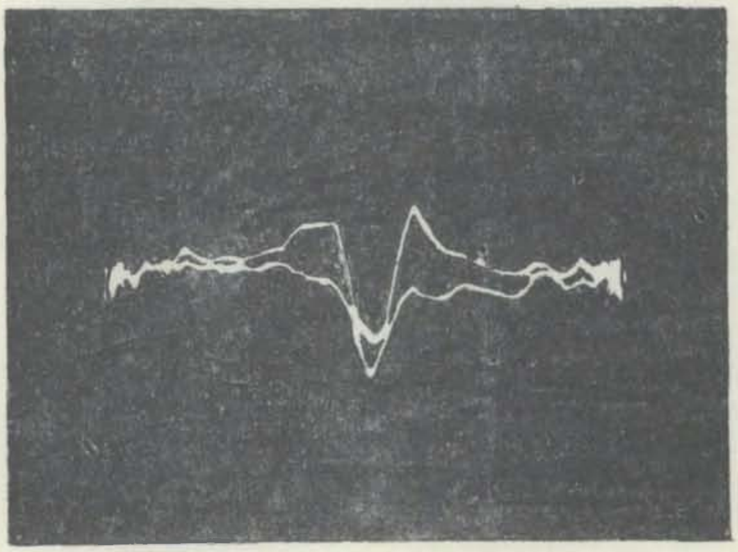

FIG. 2.

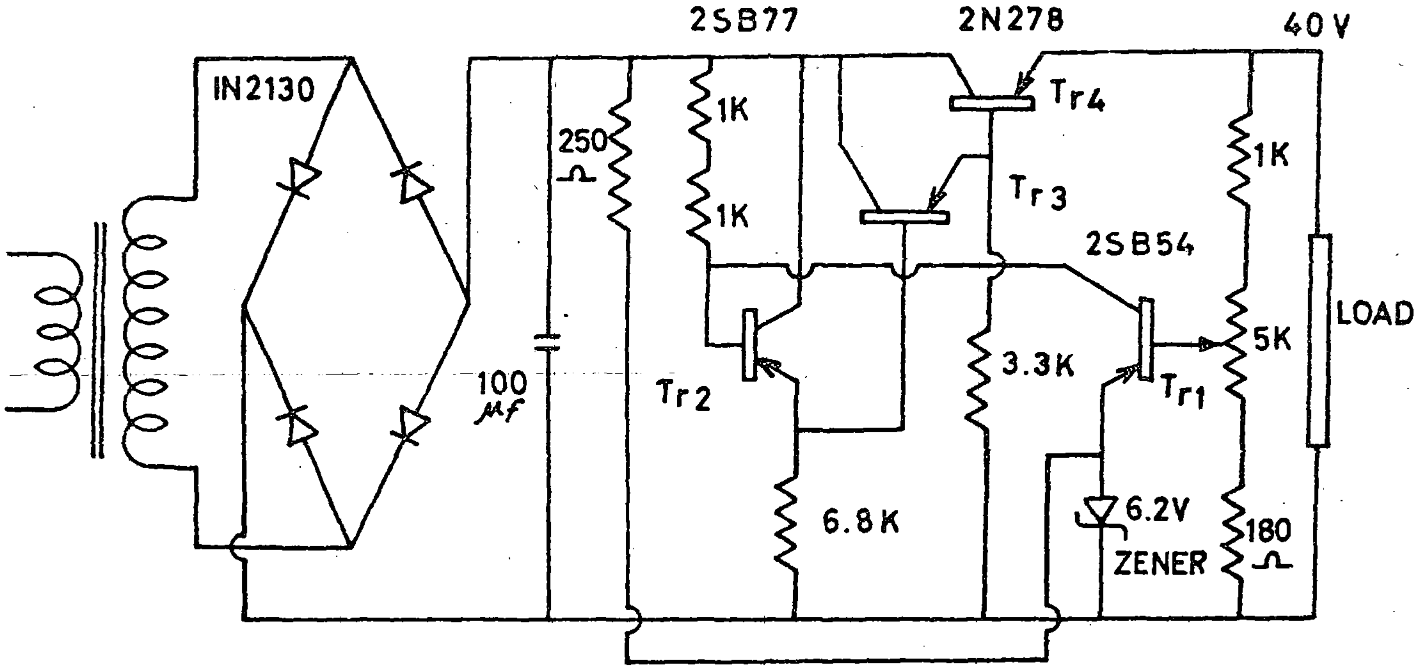

FIG. 3. STABILISED POWER SUPPLY

RESEARCH EXPERIMENTS

1. The two-nucleon stripping reaction $^{40}Ca(^{3}He, p)^{42}Sc$ - B.K. Jain and N.Sarma - The (^{3}He, p) reaction is a specially interesting reaction because the cross section for the process depends on the correlations between the captured neutron-proton pair in the final nucleus. Secondly, starting from stable even nuclei like ^{12}C, ^{16}O or ^{40}Ca, crucially important nuclei such as ^{14}N, ^{18}F and ^{42}Sc may be studied. Similar studies on the (^{3}He,n) and (t,p) reactions have been carried out by Henley and Yu[1] and others.

In this report, a ''modified zero-range'' approximation in the distorted wave formalism has been used to obtain differential cross section of (^{3}He,p) reactions, in particular the $^{40}Ca(^{3}He, p)^{42}Sc$ reaction.

Theory:

From the Gell-Mann and Goldberger[2] expression, the transition matrix element for the reaction is:

$$T = \langle \Psi_f(\xi_f)\, \chi_f^{(-)k}(K_f, y_f) + V_f \,|\, \Psi_i(\underline{\xi}_i)\, \chi_i^{(+)}(\underline{K}_i, y_i) \rangle$$

The differential cross section is given in terms of the transition matrix element

$$\frac{d\sigma}{d\Omega} = \frac{\mu_i \mu_f}{(2\pi \hbar^2)^2} \frac{K_f}{K_i} \left(\frac{1}{(2J_i+1)(2J_{pr}+1)} \right) \sum_{\substack{m_i\, m_f \\ \sigma_i\, \sigma_f}} |T|^2$$

μ and K are the reduced mass and wave number; J_i, J_{pr} are the spins of the initial nucleus and projectile with projections m_i, j_i and m_f, σf are the projections of the spins of the final nucleus (J_f) and

emergent particle (J_p). In this theory the following assumptions were made: 1) $V_f = V_{np'} + V_{pp'}$ where n and p are the captured pair and p' is the emergent particle. V_f is then assumed to have a spin and isospin independent form with a Gaussian spread in shape.
2) $\Psi_f(\xi)$, the internal wave function in the final state is written in terms of the wave functions of the initial nucleus and the captured nucleons. It is assumed for calculation that the nucleons are in a relative s-state in a harmonic oscillator potential.
3) The ^{3}He wave function is written as an antisymmetrised s-state Gaussian.
4) By assuming that the optical wavefunctions do not vary over the dimensions, ξ of the ^{3}He wavefunction the six dimensional integral reduces to a three dimensional integral. The effect of introducing a "finite range" approximation has also been investigated. Using the lc energy approximation method, the first order correction to the differe tial cross section has been calculated. This method is extremely usef in accounting for non-local potentials in addition to the finite range of the potential.

The calculations were programmed for the CDC-3600 computer of the Tata Institute of Fundamental Research. The code DWBAHE3P, calculates the differential cross section for the reaction excluding nuclear structure factors.

Results:

The optical model parameters for ^{3}He and protons on ^{40}Ca and ^{42}Sc were not available. The effect of varying these parameters was therefore investigated. (see Fig. 4). The best fit to the experimental data (see Fig.5) were obtained with values tabulated below:

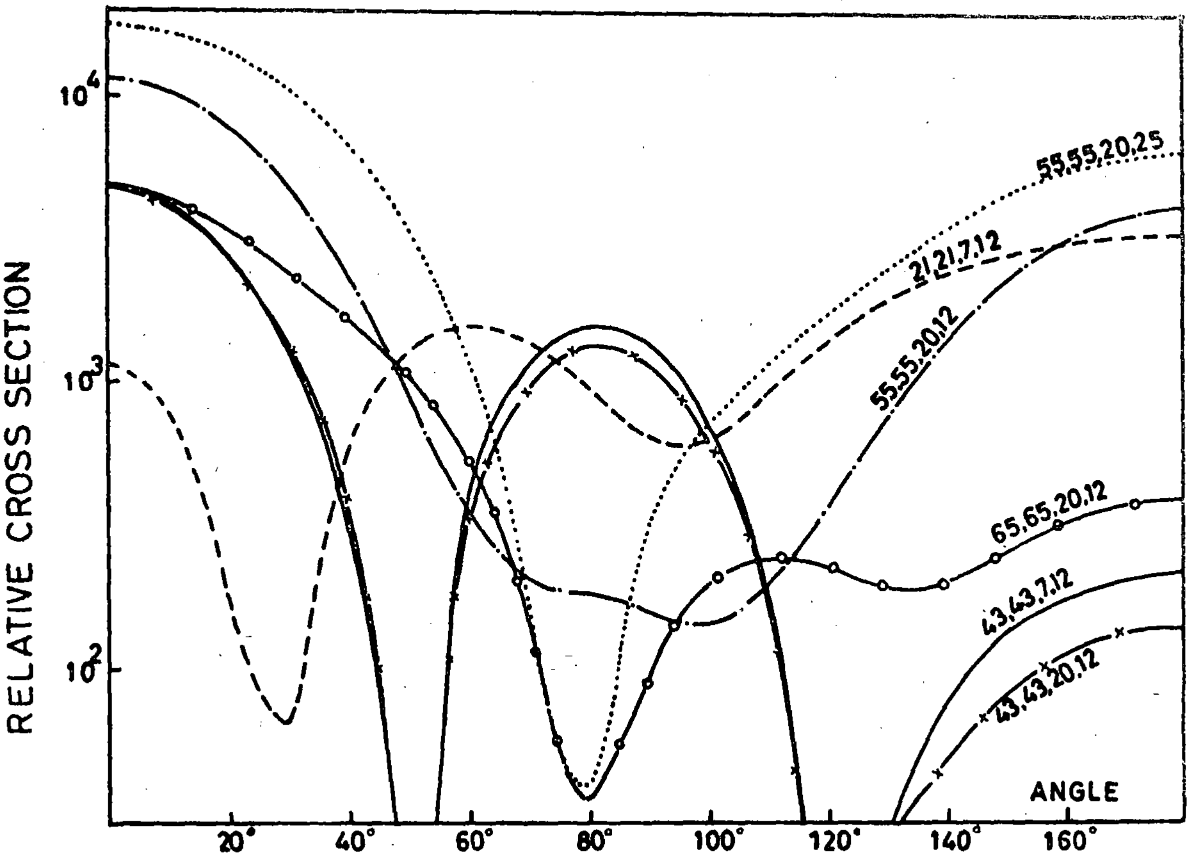

FIG.4 EFFECT OF OPTICAL POTENTIAL PARAMETERS

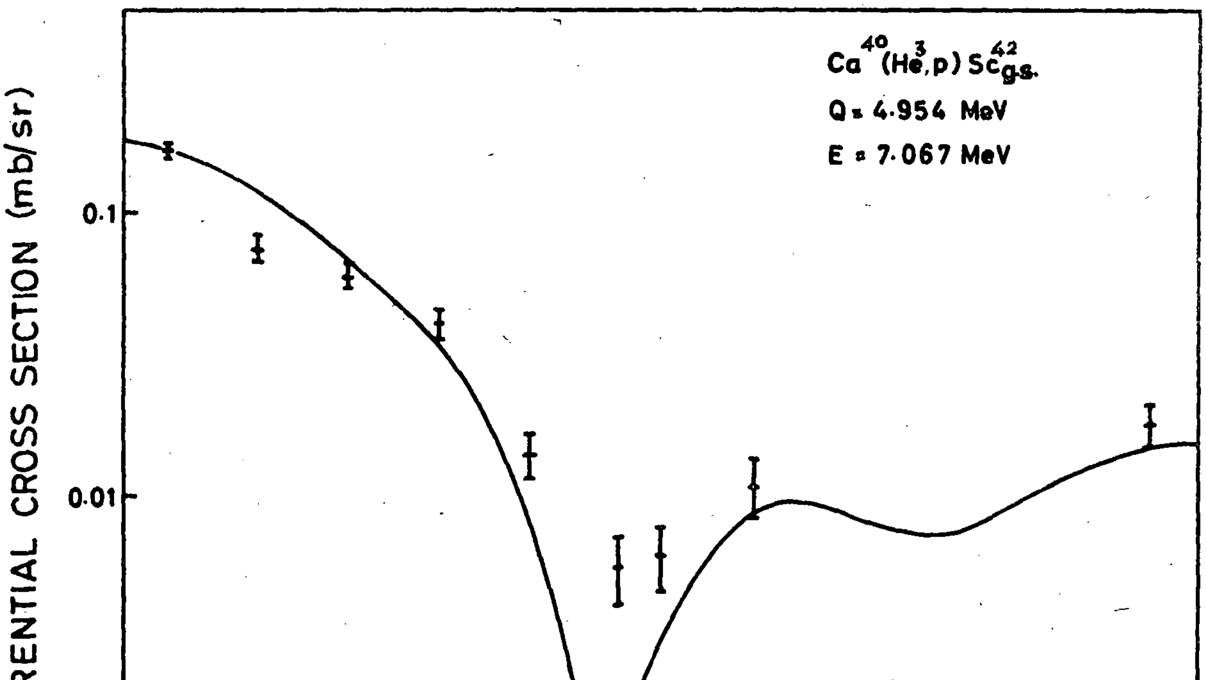

FIG.5 DWBA FIT TO THE EXPERIMENTAL DATA

TABLE

	Input	Output
V =	43 MeV (SW)	43 MeV (SW)
Radius (V)	5.472	4.345 fermi
Diffuseness (V)	0.6	0.65 fermi
W =	20 MeV (SW)	12 MeV (G)
Radius (W)	5.472	4.345 fermi
Diffuseness	0.6	0.98
Coulomb radius =	4.959 fermi	

References:

1) E.M. Henley, D.U.L.Yu, Phys. Rev. 133 B (1964) 1445.

2) M.Gellmann and Goldberger,M.L.,Phys.Rev.,91,(1953),398.

2. Spins of the first two excited states in ^{27}Mg by proton gamma ray angular correlation measurements in the reaction ^{26}Mg(d, p γ)^{27}Mg - M.A. Eswaran - Many nuclei in the 2s - 1d shell have been extensively studied and the properties of low lying excited states have been compared with the predictions of various nuclear models[1]. ^{27}Mg, however, has received relatively little attention. In the work reported here, the first two excited states of ^{27}Mg at 0.98 and 1.69 MeV have been studied by proton-gamma ray angular correlation measurements in the reaction ^{26}Mg(d, p γ)^{27}Mg employing the Litherland and Ferguson[2] method in which the analysis is independent of any assumption

regarding the reaction mechanism.

Deuteron beam of 1.8 MeV energy from the Van de Graaff Accelerator was used to populate the levels in the ^{27}Mg in the reaction $^{26}Mg(d, p\gamma)^{27}Mg$. A separated isotope target of ^{26}Mg ($\sim$100 ug/cm^2) on tantalum backing was used, mounted at the centre of a cylindrical brass target chamber of 15 cm. diameter. The incoming deuteron beam was collimated by two tantalum apertures 25 cm apart the first one with 1.5 mm dia. and second with 2 mm dia. and the beam was stopped by the tantalum target backing. The protons from the reaction were detected at zero degree to the beam in a surface barrier silicon detector subtending a half angle of 4° at the target. Gamma rays were detected in a 4.4 cm dia x 5 cm long NaI (Tl) scintillation detector. The gamma ray detector with its associated lead shielding was mounted on an arm which can rotate with respect to the vertical axis passing through the beam spot on the target in the target chamber.

Gamma ray spectra were recorded in coincidence with the proton using a fast-slow coincidence system with a resolving time $2\tau = 100$ nanoseconds and random coincidence spectrum was also recorded simultaneously using another identical coincidence system with a large delay introducted in one of the fast channels. Recording of gamma ray coincidence spectra in coincidence with the selected proton groups feeding a particular excited state in the residual nucleus in the reaction were carried out using the two parameter analysing facility which incorporates a 20 channel pulse height analyser in conjunction with a TMC 400 channel analyser. Proton gamma ray angular correlation measurements were made selecting the proton groups feeding the first and second excited states ^{27}Mg successively in the gating window in the coincidence system. Fig. 6a shows the direct proton spectrum and Figs. 6b and 6c show the gamma ray spectra in coincidence with P_1 and P_2 groups from the reaction $^{26}Mg(d, p\gamma)^{27}Mg$. For each set of angular correlation data coincidence spectra were recorded at seven angles of gamma detector position from 0° to 90° in steps of 15°. Figs. 7a and 7b show the $p_1 - \gamma_{0.98}$ and $p - \gamma_{1.69}$ MeV angular correlations respectively. Least squares fit analysis of the $p_1 - \gamma_{0.98}$ MeV angular correlation data with even order Legendre polynomial functions upto and including P_4 gives:

$$W(\theta) = 1 - (0.12 \pm 0.07) P_2(\cos\theta) - (0.09 \pm .09) P_4(\cos\theta) \qquad \ldots 1$$

A second set of measurements was also taken on P_1 - gamma angular correlation with slightly different target thickness and this set yields a least squares fit of

$$W(\theta) = 1 - (0.09 \pm 0.05) P_2(\cos\theta) - (0.01 \pm 0.06) P_4(\cos\theta) \qquad \ldots 2$$

For $p_2 - \gamma_{1.69}$ MeV correlation the least squares fit was obtained as

$$W(\theta) = 1 + (0.37 \pm .07) P_2(\cos\theta) - (0.27 \pm .08) P_4(\cos\theta) \qquad \ldots 3$$

For the geometry of gamma detector used, the correlation attenuation factors due to the finite detector size are Q_2 = .981 and Q_4 = 0.936.

From the (d, p) reaction angular distribution studies[1] the angular momentum l_n values of captured neutron are given as 2 for both the first and second excited states in ^{27}Mg implying positive parity and spin values of 3/2 or 5/2 for both the states. The ground state spin of ^{27}Mg is known[1] to be $1/2^+$. As shown by Litherland and Ferguson[2] (method II) if the outgoing particles are detected at 0° with respect to the beam in a small axially symmetric detector and the correlation of subsequent de-excitation gamma ray from the excited state in the residual nucleus is measured then the magnetic substates which can be populated in the excited state are limited by the sum of the spins of target nucleus, bombarding and outgoing particles. Accordingly the present reaction $^{26}Mg(d, p\gamma)^{27}Mg$ only the 1/2 and 3/2 substates are populated in the state excited in ^{27}Mg. Higher substates can be populated to a small extent due to the effect of the finite size of the proton detector. In terms of the magnetic substate population parameters P(m), the angular correlation[2,3] of $5/2^+$ $1/2^+$ quadrupole transition can be written as

$$W(\theta) = \left[P(\tfrac{1}{2}) + P(\tfrac{3}{2}) + P(\tfrac{5}{2})\right] + \left[\tfrac{4}{7} P(\tfrac{1}{2}) + \tfrac{1}{7} P(\tfrac{3}{2}) - \tfrac{5}{7} P(\tfrac{5}{2})\right] Q_2 P_2 \cos\theta + \left[\tfrac{4}{7} P(\tfrac{1}{2}) + \tfrac{6}{7} P(\tfrac{3}{2}) - \tfrac{2}{7} P(\tfrac{5}{2})\right] Q_4 P_4 \cos\theta \quad \ldots 4$$

It is seen from Equation (4) that when the population is limited to 1/2 and 3/2 substates of the excited state of spin 5/2 then 5/2 $\rightarrow$ 1/2 quadrupole transition gamma ray can have only positive coefficient for the $P_2(\cos\theta)$ term in the angular correlation. It is also observed from the above equation that the contribution of negative coefficient for $P_2(\cos\theta)$ term due to the small population of 5/2

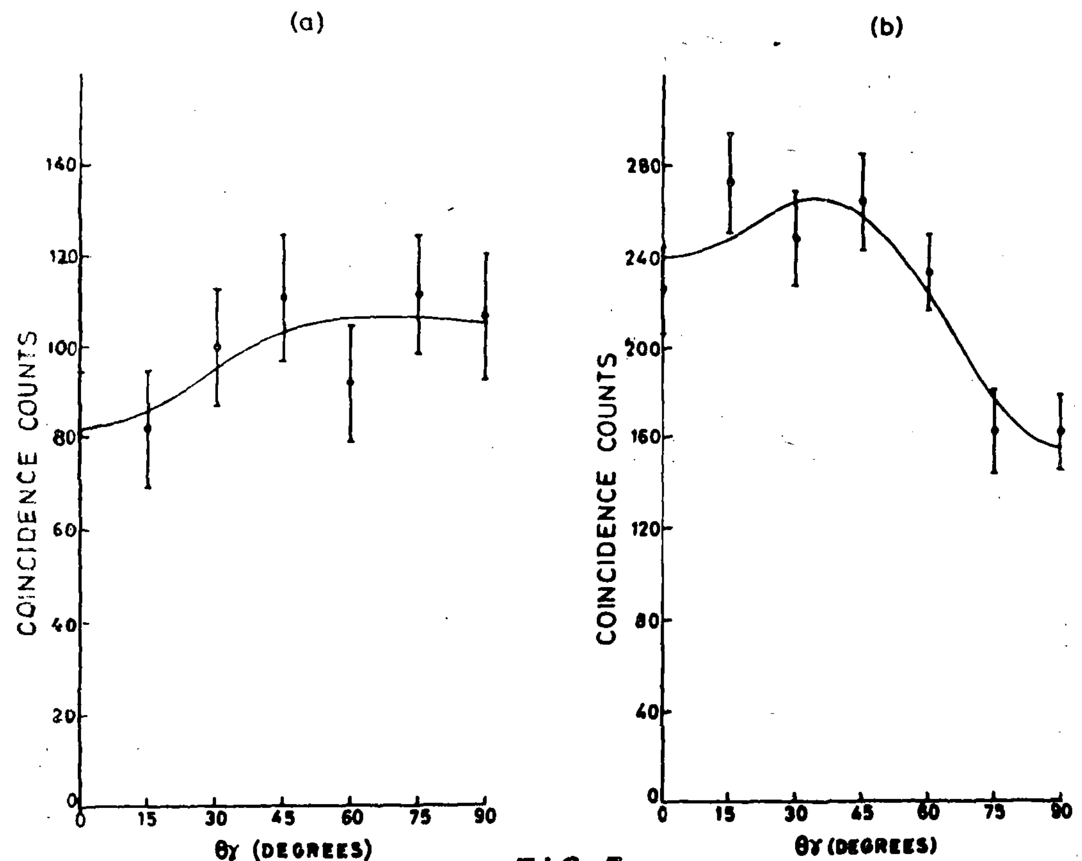
(a)
COINCIDENCE COUNTS
0
20
40
60
80
100
120
140
0
15
30
45
60
75
90
θγ (DEGREES)
(b)
COINCIDENCE COUNTS
0
40
80
120
160
200
240
280
0
15
30
45
60
75
90
θγ (DEGREES)

FIG. 7.

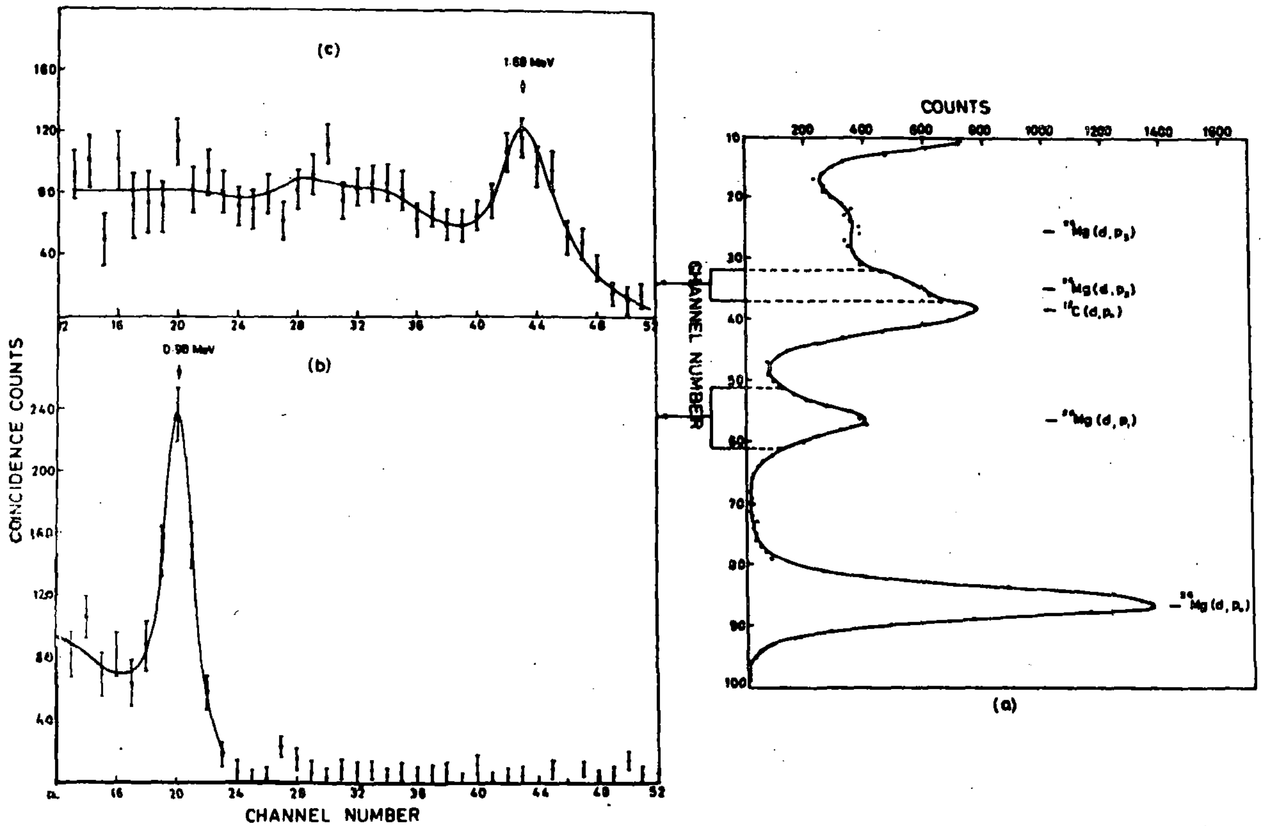
(c)
1.69 MeV
(b)
0.98 MeV
COINCIDENCE COUNTS
CHANNEL NUMBER
COUNTS
(a)

FIG. 6.

substate owing to the finite proton counter size, cannot offset the positive contribution due to the predominant 1/2 and 3/2 substates. Hence from the observed negative coefficient for $P_2(\cos\theta)$ term in correlation for the 0.98 MeV gamma ray from the first excited state to the ground state and the zero $P_4(\cos\theta)$ term within experimental errors as seen from Equation (1) and (2) the 0.98 MeV first excited state can be assigned the spin of 3/2 ruling out 5/2. For the second excited state at 1.69 MeV spin of 5/2 can be assigned ruling out 3/2 from the observed (Equation 3) significant $P_4(\cos\theta)$ term in the correlation.

The second excited state at 1.69 MeV of ^{27}Mg is found to decay almost completely to the ground state as in the case of other Z or N = 15 nuclei ^{31}P and ^{29}Si which are also having the spin sequence of 1/2, 3/2 and 5/2 for the ground, first and second excited states. Further studies in the reaction $^{26}Mg(d, p\gamma)^{27}Mg$ are in progress to obtain information about the higher excited states in ^{27}Mg.

References:

1) P.M. Endt and C. Van der Leun, Nuclear Phys. 34 (1962) 1.
2) A.E. Litherland and A.J.Ferguson, Can. J. Phys. 39 (1961) 788.
3) W.T. Sharp et al., AECL Report No. 97.

3. Elastic scattering of alpha particles from ^6Li - D.K. Sathe, K.B. Nambiar, A.S.Divatia and M.K. Mehta - The elastic scattering of alpha particles from ^6Li has previously been observed from E_α = 0.9 to 2.7 MeV corresponding to excitation energies in ^{10}B of 5.1 to 6.2 MeV by Dearnaley[1] et al. for studying the levels in ^{10}B. They obtained resonance structures for the 5.18 and the 5.92 MeV levels in ^{10}B. In

the present work levels in ^{10}B lying between 5.92 MeV and 7.01 MeV have been investigated by studying the elastic scattering of alpha particles from ^{6}Li for incident alpha particle energies from 2.4 to 4.5 MeV.

Thin targets of ^{6}Li deposited on carbon film (approximately 10 ugm/cm^2 thick) were bombarded with singly charged helium ions obtained from the 5.5 MeV Van de Graaff Accelerator. Elastically scattered alpha particles were observed at two angles $\theta_{c.m} = 87.5°$ and $\theta_{c.m} = 121°$ corresponding to $\theta°$(Lab)= 56° and $\theta°$(Lab)= 80°, respectively, using ORTEC solid state detectors. The scattering chamber used has been previously described[2]. Pulses from the detectors after suitable amplification were fed into a TMC 400 channel analyser. The alpha beam, after it had passed through the target, was stopped in a Faraday cup and the current integrated. A typical spectrum obtained with the TMC 400 channel analyser is shown in Fig. 8. The energy steps for the excitation curves varied from 7 to 14 KeV. Excitation curves at the two angles are shown in Fig. 9. Resonance structures are seen at E_{α}(Lab) = 2.45, 2.68, 2.87, 3.11, 3.51 and 4.34 MeV corresponding to excited levels in the compound nucleus ^{10}B at 5.93, 6.06, 6.18, 6.31 6.57 and 7.05 MeV. The level at 6.31 MeV has not been previously reported[3,4]. There is an indication of an anomaly at E_{α}(Lab) = 3.93 MeV, implying a level in ^{10}B at 6.81 MeV.

The anomaly at E_{α}(Lab) = 3.51 MeV corresponding to the 6.56 MeV level in ^{10}B shows an interesting behaviour at the two angles. The level appears well isolated from neighbouring levels. It should therefore be possible to determine its spin and parity by the application of single level resonance theory. With this objective, angular distribut

$^{6}Li(\alpha,\alpha)^{6}Li$ SPECTRUM AT $E_{\alpha} = 3.515$ MeV

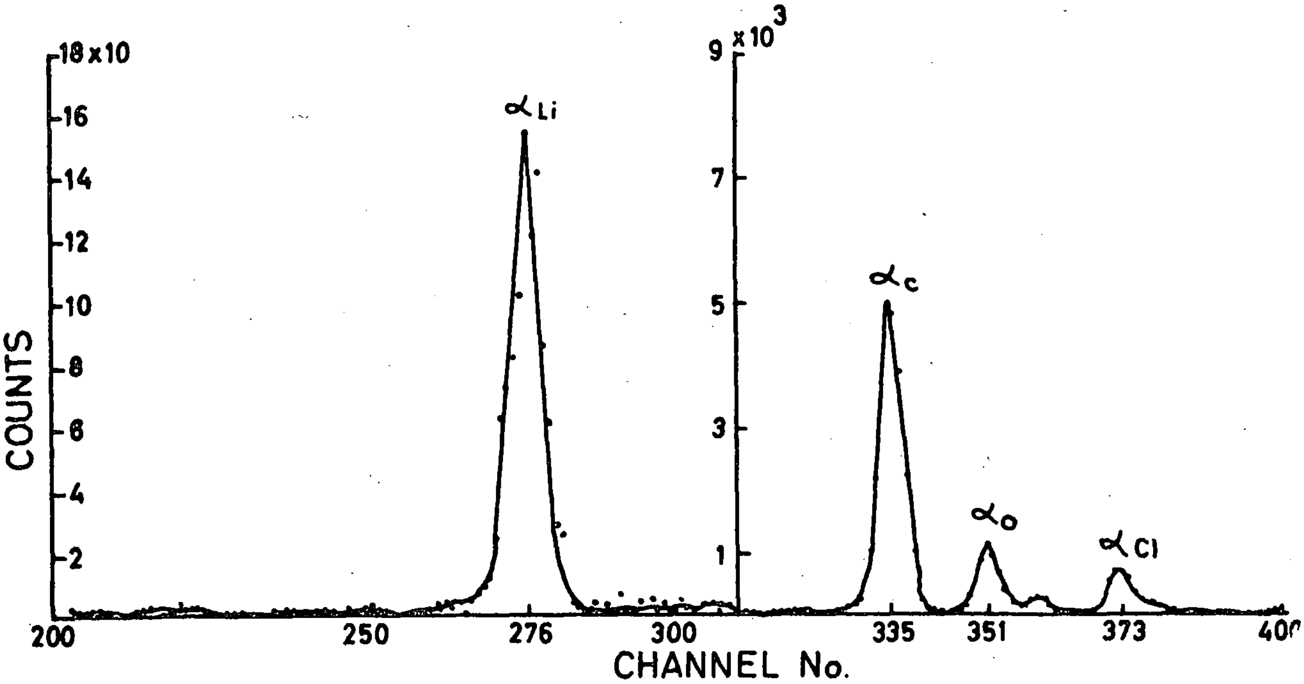

FIG. 8.

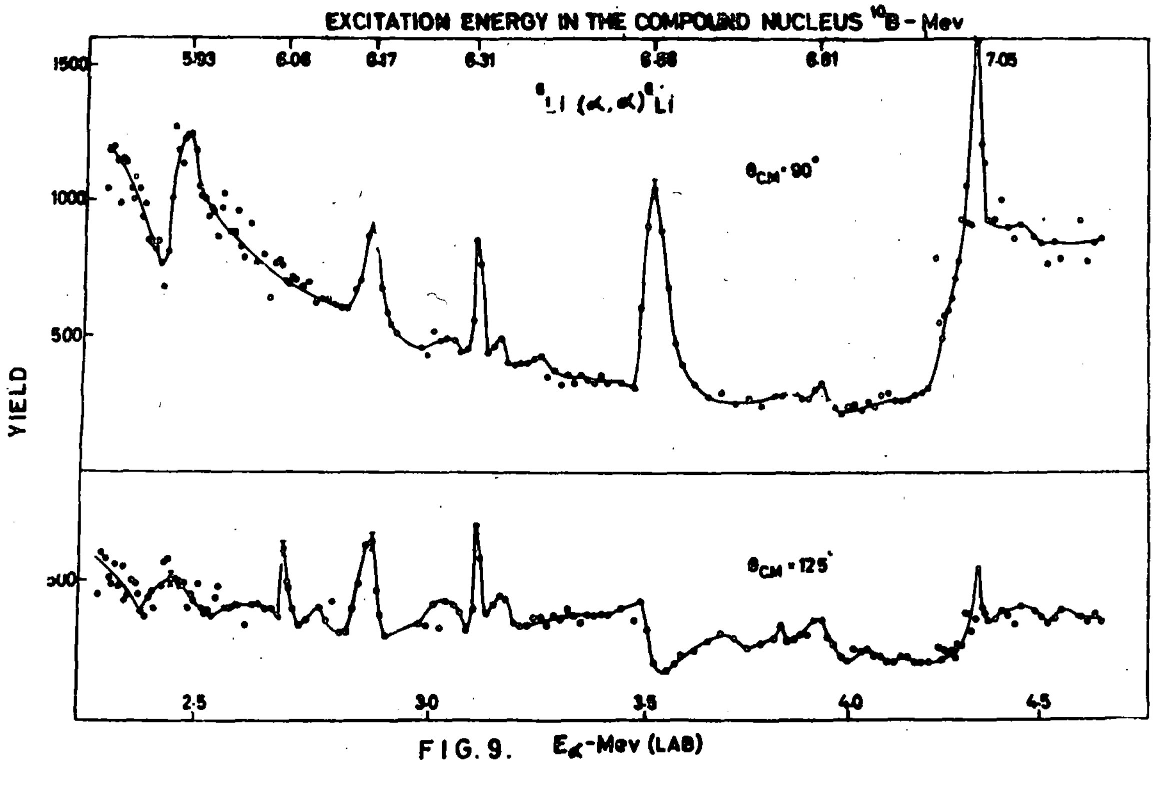

FIG. 9. E_{α}-Mev (LAB)

of the elastically scattered alpha particles were obtained over the resonance at 3.51 MeV.

References:

1). G.Dearnaley, D.S.Gammel and S.S.Hanna, Nuclear Phys. 36 (1962) 71.

2) N.Sarma, K.S.Jayaraman and C.K.Kumar, Nuclear Phys. 44 (1963) 205.

3) F.Ajzenberg Selove and T.Lauritsen, Nuclear Phys. 11 (1959) 79.

4) P.P.Singh and D.S.Gemmel, Bull.Amer.Phys. Soc. Ser.II No. 4 (1965) 538.

4. Fluctuation analysis of $^{27}Al(p, \alpha_0)^{24}Mg$ and $^{27}Al(p, p_3')^{27}Al^*$ cross sections - M.K. Mehta and A.S.Divatia - Fluctuation theory has been applied to the cross sections for the reactions $^{27}Al(p, \alpha_0)^{24}Mg$ and $^{27}Al(p, p_3)^{27}Al^*$ [1]. The excitation curves taken at $\theta_{lab} = 90°$ and 150° extended from E = 4.00 to 5.50 MeV, corresponding to excitation energies between 15.0 and 16.5 MeV in the compound nucleus ^{28}Si. At such excitations the level density is expected to be high enough so that the ratio of average level width Γ to the average level separation D is greater than unity, and fine resolution excitation curves are expected to exhibit Ericson fluctuations. The structure exhibited by the two excitation curves should then be statistically independent.

The fluctuation theory has been worked out by Ericson[2], Brink, Stephen[3] and others and is now at such a stage that useful information about the reaction mechanism and the average life time of the compound nucleus can be extracted by its application. Criteria for the validity of such analysis for individual cases are not yet clearly established.

In the theory the autocorrelation function for a curve is defined as

$$C(\epsilon) = \frac{\Delta E}{E_2 - E_1} \sum_{E=E_1}^{E_2} \left(\frac{\sigma(E)}{\langle\sigma(E)\rangle} - 1\right)\left(\frac{\sigma(E+\epsilon)}{\langle\sigma(E+\epsilon)\rangle} - 1\right)$$

where E is the interval between successive measurements taken over the range $E_1 \leq E \leq E_2$ and $\epsilon = n \Delta E$ where n is an integer.

For the autocorrelation function for $\epsilon \leq \Gamma$ the theory predicts

$$C(\epsilon) = C(0) \frac{\Gamma^2}{\Gamma^2 + E^2}$$

The cross correlation function between two curves a and b is defined as

$$C_{ab}(\epsilon) = \frac{\Delta E}{E_2 - E_1} \sum_{E=E_1}^{E_2} \left(\frac{\sigma_a(E)}{\langle\sigma_a(E)\rangle} - 1\right)\left(\frac{\sigma_b(E+\epsilon)}{\langle\sigma_b(E+\epsilon)\rangle} - 1\right)$$

The quantity $C_{ab}(0)$ should be very small if the fluctuation interpretation is valid.

The averaging interval δ over which the averaging $\langle\ \rangle$ is performed should be large enough to average over several Γ's. The correlation functions would be insensitive to any increase in δ after that.

Denoting the curves for the reactions $^{27}Al(p, \alpha_o)^{24}Mg$ at $\theta_{lab} = 90°$ and $\theta_{lab} = 150°$ by numbers 1 and 2 respectively, and that for the reaction $^{27}Al(p, p_3)^{27}Al^*$ at 90° by number 3, the quantities $C_1(\epsilon)$, $C_{12}(\epsilon)$ and $C_{13}(\epsilon)$ were calculated for δ ranging from 20 to 1500 KeV in steps of 50 KeV, utilising the CDC 3600 computer. Results are shown in Fig. 10. From Fig. 10a, it is seen that for $\delta > 300$

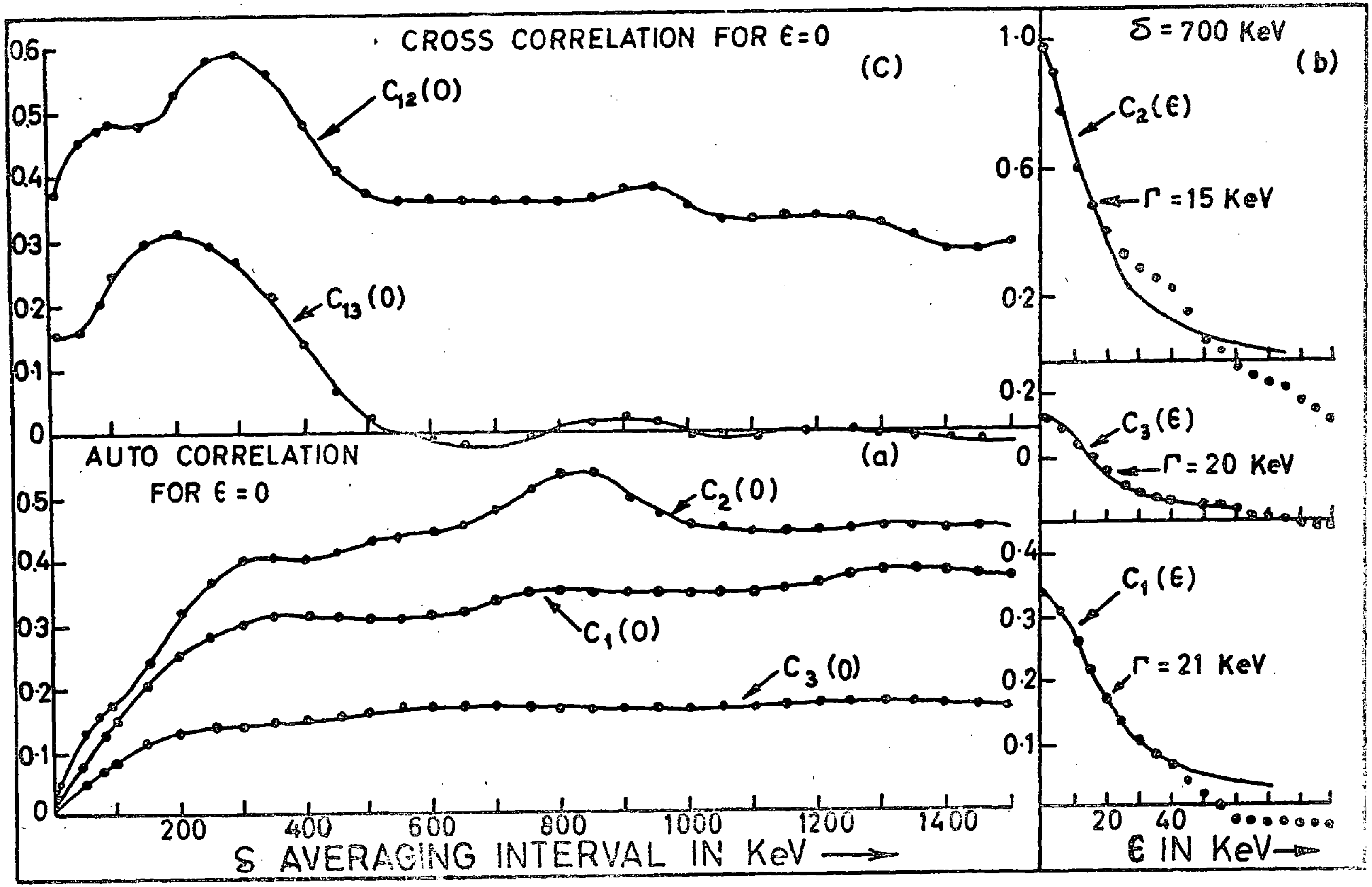

CROSS CORRELATION FOR ϵ=0
(C)
$C_{12}(0)$
$C_{13}(0)$
AUTO CORRELATION FOR ϵ = 0
(a)
$C_2(0)$
$C_1(0)$
$C_3(0)$
S AVERAGING INTERVAL IN KeV
δ = 700 KeV
(b)
$C_2(\epsilon)$
Γ =15 KeV
$C_3(\epsilon)$
Γ = 20 KeV
$C_1(\epsilon)$
Γ = 21 KeV
ϵ IN KeV

FIG. 10.

KeV the curves are approximately flat as expected. Fig. 10b shows the quantities $C_1(\epsilon)$, $C_2(\epsilon)$ and $C_3(\epsilon)$ for δ = 700 KeV. The lines shown are Lorentzian fits calculated for the appropriate Γ. Thus if the fluctuation interpretation is valid, the Γ for the compound nucleus ^{28}Si at an excitation between 15.0 and 16.5 MeV ranges from 14 to 22 KeV, depending on δ and the excitation curve.

In Fig. 10c the cross correlations $C_{12}(0)$ and $C_{13}(0)$ show a peak. Curves 1 and 2 are for the same reaction at two different angles and according to Brink, Stephen and Tanner[4] the structure in such a case would be correlated only if $(\theta_1 - \theta_2) \leq \frac{1}{kR}$ where k is the momentum and R is the interaction radius. Here $(\theta_1 - \theta_2) = 58°$ while $\frac{1}{kR} \sim 32°$. Thus the cross correlation should be very small, which is certainly not the case.

Although a value of Γ = 20 KeV can be extracted by the fluctuation analysis, the large cross correlation between curves 1 and 2 for all δ's and between curves 1 and 3 for some δ suggest that, besides the contribution due to fluctuations, the structure shown by the three excitation curves represents resonance effects due to separate but interfering levels in the compound nucleus ^{28}Si. In this analysis, one can perceive the importance of measuring data with fine resolution and choosing the appropriate value of the averaging interval δ.

<u>References:</u>

1) Joseph John, S.S.Kerekatte, M.K.Mehta, Proc. of Nuclear Physics and Solid State Physics Symposium, part - Nuclear Physics, Dept. of Atomic Energy, Government of India (1965) p. 194.

2) T.Ericson, Annals of Physics <u>23</u> (1963) 390.

3) D.M.Brink and R.P.Stephen, Phys. Lett. <u>5</u> (1963) 77

4) D.M.Brink, R.P.Stephen and N.W.Tanner, Nuclear Phys. <u>54</u> (1964) 577.

5. <u>Study of the $^{51}V(p, n)^{51}Cr$ reaction</u> - K.V.K.Iyengar@, S.K.Gupta@ and B.Lal@ - Measurement of angular correlations of the emitted nucleons and gamma rays from the residual nucleus is a very sensitive method of studying the reaction mechanism. CN and DI mechanisms predict different types of symmetry for the particle-gamma angular correlations. The measurement of n- γ correlations in the reaction $^{51}V(p, n\gamma)^{51}Cr^*$ and the excitation functions of the gamma rays was performed to investigate the mechanism of the reaction.

The excitation functions of the 0.75, 1.17, 1.35 and 1.50 MeV gamma rays from the reaction $^{51}V(p, n)^{51}Cr$ were measured from their respective thresholds to 5.5 MeV in steps of 50 KeV using a natural vanadium target of thickness 1.2 mg/cm^2. The excitation functions are presented in Figs. 11, 12 and 13. The shaded triangles in above figures represent the energy spread as a function of proton energy due to target thickness. They exhibit no significant structure. The ratio of the intensities of 0.75 and 1.17 MeV gamma rays as a function of proton energy was calculated according to Hauser-Feshbach theory using Satchler's formalism for various assumed values of the spins for the 0.75 and 1.17 Me levels of ^{51}Cr. Since according to the single particle shell model the states available for ^{51}Cr in the region of low excitation have all negativ parities, the parities of the levels were assumed to be negative. The compound nucleus ^{52}Cr was assumed to decay through the (p, n) reaction only and only to the ground state and the first two excited states of ^{51}Cr No account was taken of the contribution to the intensity of 0.75 and

---

@ Tata Institute of Fundamental Research , Bombay.

EXCITATION FUNCTION OF 0·75 AND 1·17 MeV GAMMA RAYS IN THE REACTION $^{51}V(p,n)^{51}Cr$

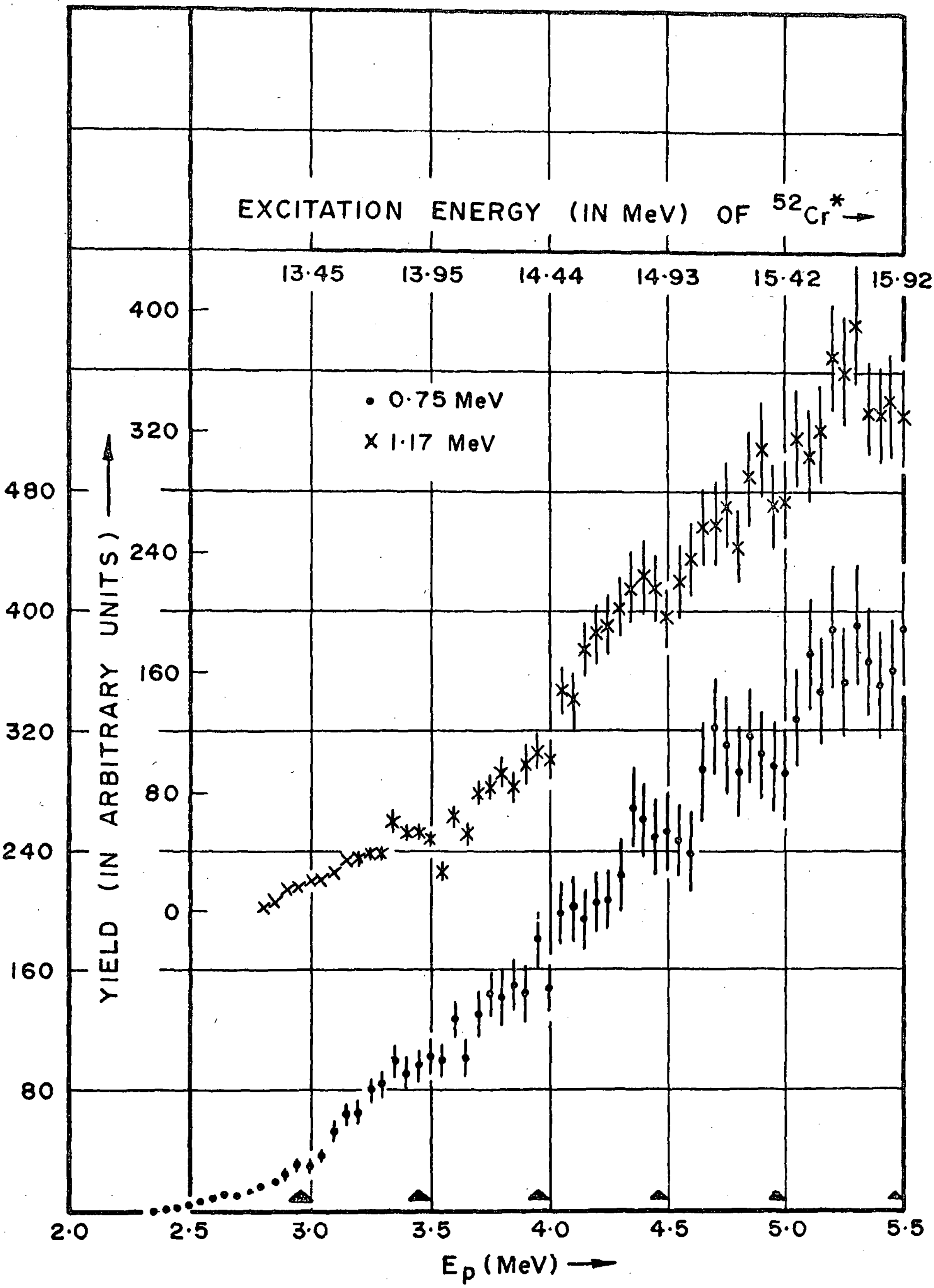

FIG. 11.

EXCITATION FUNCTION OF 1·35MeV GAMMA RAYS IN THE REACTION $^{51}V(p,n)^{51}Cr$

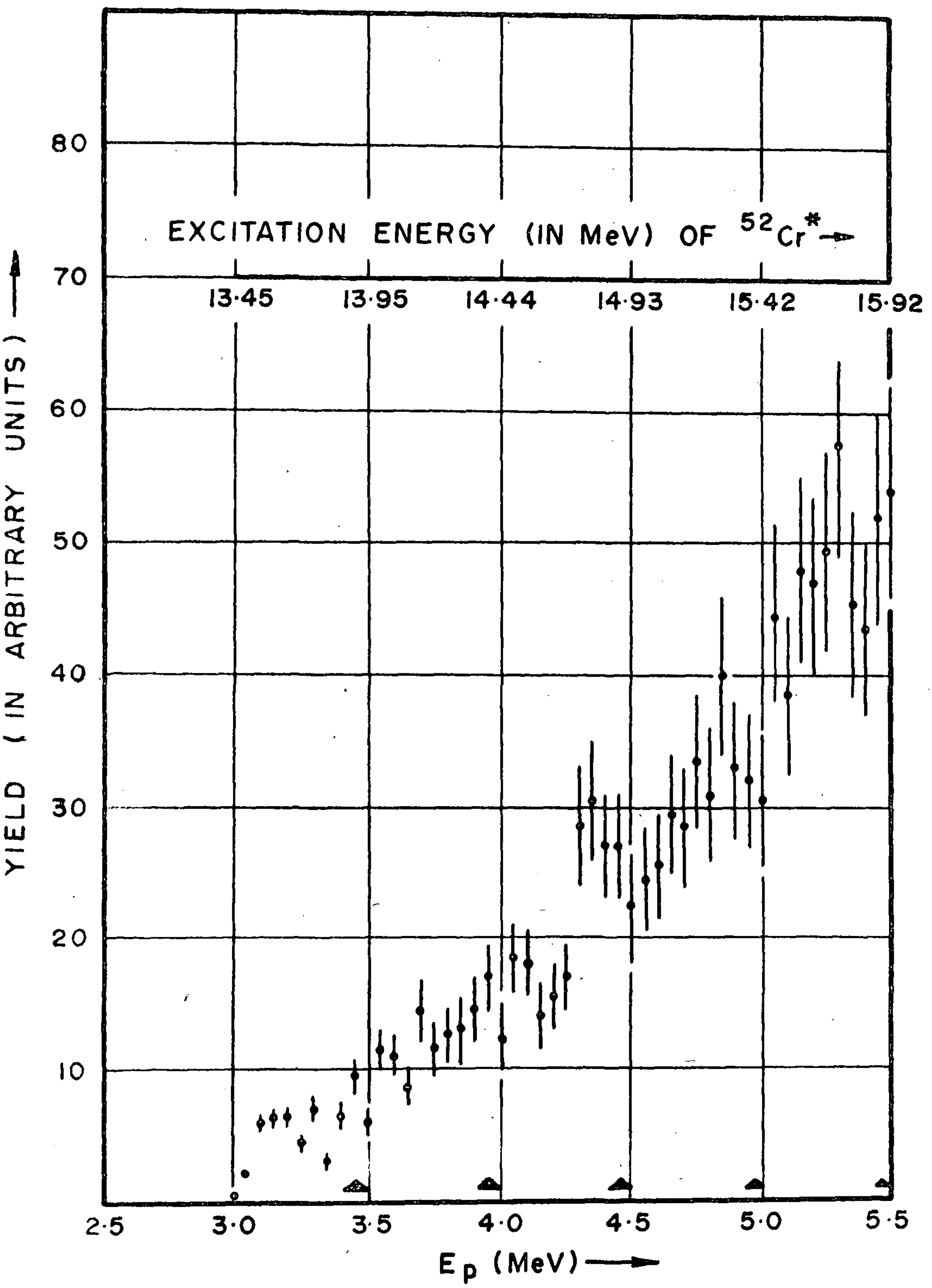

FIG.12.

EXCITATION FUNCTION OF 1·50 MeV GAMMA RAYS IN THE REACTION $^{51}V(p,n)^{51}Cr$

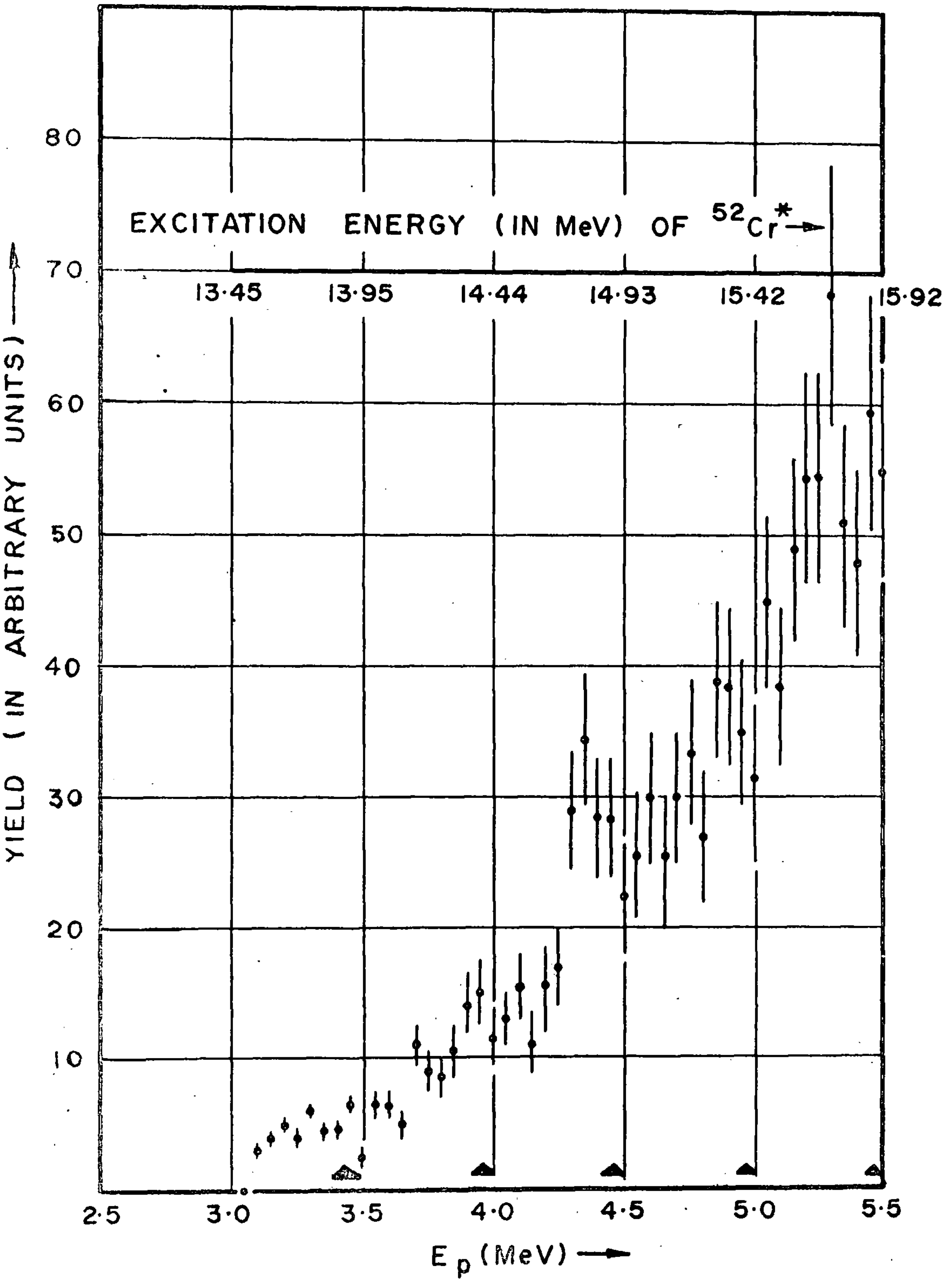

FIG. 13.

1.17 MeV gamma rays by the decay of higher levels through these two levels as no detailed information on the branching ratios of the different decay modes of higher levels was available. However, it is well established that the level at 1.17 MeV deexcites by a direct transition to ground state. The proton and neutron transmission coefficients at the desired energies were obtained by linear interpolation from the tables of Mani et al.[2, 3]. The observed and calculated ratios of the intensities of the 0.75 and 1.17 MeV gamma rays are presented in Fig. 14. The theoretical curves exhibit a valley and a peak in the proton energy region 3.0 to 4.0 MeV which are not genuine and result from the linear interpolation procedure adopted to derive transmission coefficients from the tables of Mani et al. It is seen that the agreement between the observed and calculated ratios is best when the spin assignment to the 0.75 and 1.17 MeV levels are 3/2 and 5/2 respectively. This assignment is in complete agreement with the assignment of Ferguson et al.[4] based on the study of the intensity of the neutron groups to ground state and the first two excited states.

It is concluded from the above that the Hauser-Feshbach statistical model is applicable for this reaction and that the spins of the 0.75 and the 1.17 MeV levels are 3/2 and 5/2 respectively.

$n_1 - \gamma$ and $n_2 - \gamma$ correlations were measured at $E_p = 3.1$ and 3.3 MeV both in the plane of (p, n) reaction and in the plane perpendicular to it. The same correlations were also measured at E_p = 3.5 MeV, but only in the plane of (p, n) reaction. The angular correlations at supplementary neutron angles were measured simultaneously by moving the gamma detector in the plane perpendicular to the (p, n) reaction plane. Vanadium targets of thickness 2.1 mgm/cm^2(on gold backing) were used for the n- γ correlation measurements. Gamma rays were detected using a NaI scintillator and neutrons were detected using plastic scintillators. The neutron groups n_1 and n_2 were resolved by time of flight technique using the gamma coincident with the neutrons as the timing pulse. A block diagram of the electronics is presented in Fig. 15 and a typical neutron time-of-flight spectrum in Fig. 16. The areas under the neutron peaks were determined by non-linear least square fitting a function of number of gaussians equal to the number of peaks seen in the spectrum plus a constant background treating the peak positions, their half widths, peak amplitudes and the intensity of the background as parameters to be determined. A Fortran programme "MINIMA" for CDC 3600 was developed to minimise χ^2 for such a function. The experimental correlations are presented in Figs. 17 and 18.

$n_1 - \gamma$ and $n_2 - \gamma$ correlations were calculated assuming the validity of the CN statistical model according to Sheldon[5)] using the Fortran programme "Pushpa" written for CDC 3600. The theoretical correlations turn out to have an anisotropy less than 2% when the emitted gamma radiations are assumed for the level from which the gamma ray is emitted.

The experimental data are not yet completely analysed. Only the data at 3.1 MeV in the $\phi = 90°$ plane has been analysed and the correlations show an anisotropy greater than the theoretically calculated ones. However, it must be borne in mind that the statistical errors on the measured points are of the order of 8%. The experimental $n_2 - \gamma$ correlations are nearly isotropic and those at supplementary angles have the same shape. The same cannot be said of $n_1 - \gamma$ correlations.

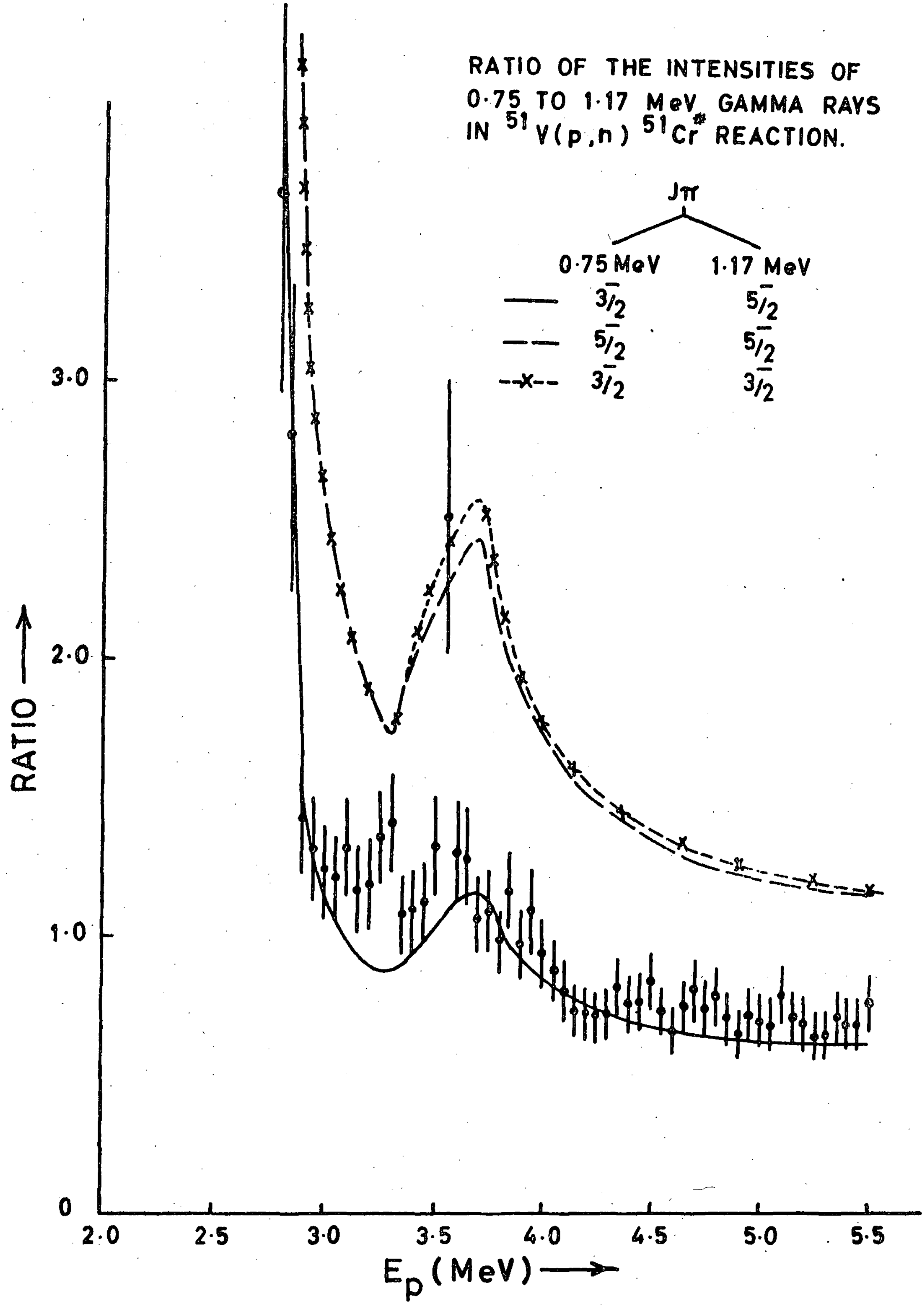
RATIO OF THE INTENSITIES OF
0·75 TO 1·17 MeV GAMMA RAYS
IN $^{51}V(p,n)\,^{51}Cr^{*}$ REACTION.
Jπ
0·75 MeV
1·17 MeV
$3/2^-$
$5/2^-$
$5/2^-$
$5/2^-$
$3/2^-$
$3/2^-$
RATIO ⟶
E_p (MeV) ⟶
0
1·0
2·0
3·0
2·0
2·5
3·0
3·5
4·0
4·5
5·0
5·5

FIG.14

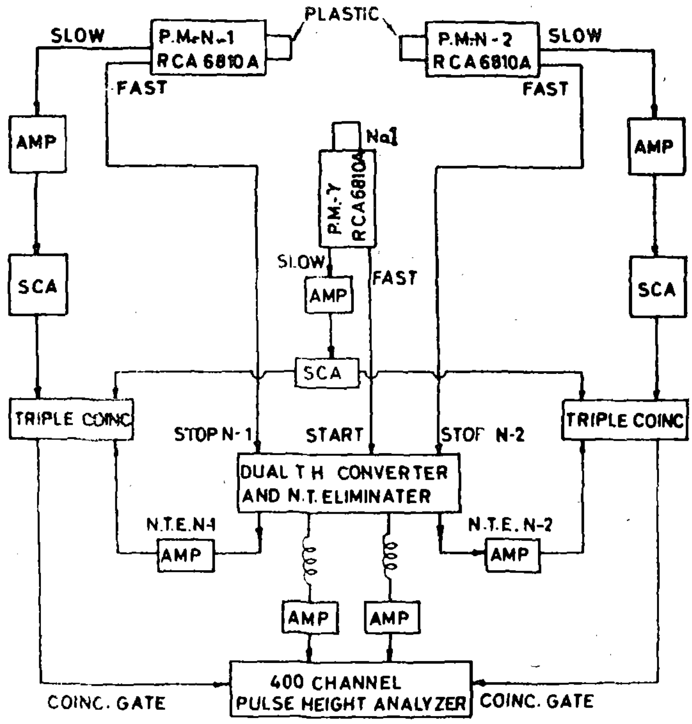

FIG.15

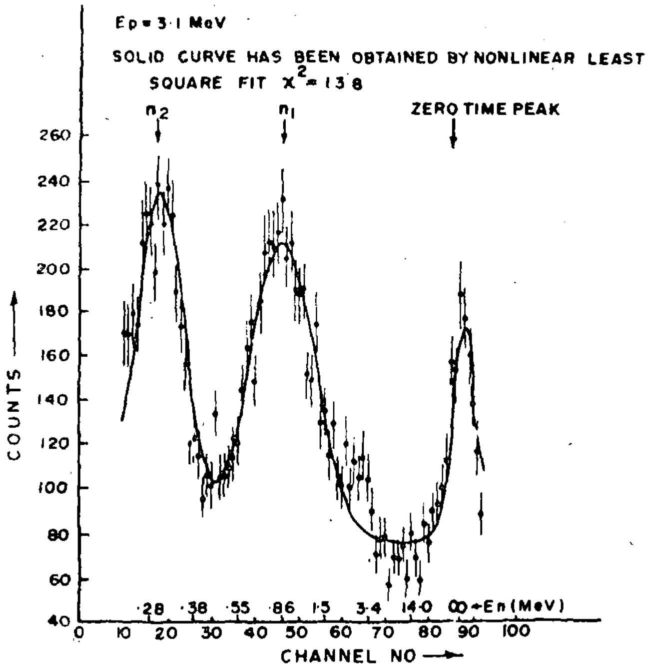

TIME OF FLIGHT SPECTRUM OF NEUTRONS IN $V^{51}(p,n)Cr^{51}$

FIG. 16.

The angular correlation in $^{51}V(p,n_1\gamma_{0.75})^{51}Cr$ at $E_p = 3.1$ MeV in $\phi = 90°$ plane. The correlations at $\theta_n = 35°$, 45° and 60° were obtained with one of the neutron detectors and those at $\theta_n = 145°$, 135° and 120° were obtained with the other neutron detector.

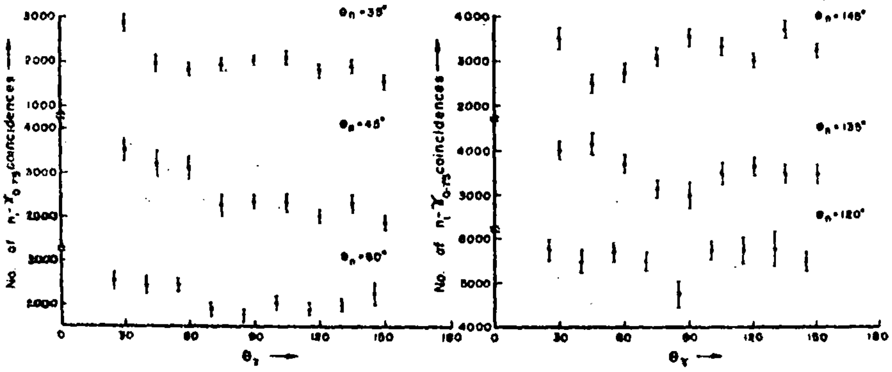

FIG. 17

The angular correlation in $^{51}V(p,n_2\gamma_{1.17})^{51}Cr$ at $E_p = 3.1$ MeV in $\phi = 90°$ plane. The correlation at $\theta_n = 35°$, 45° and 60° were obtained with one of the neutron detectors and those at $\theta_n = 145°$, 135° and 120° were obtained with the other neutron detector.

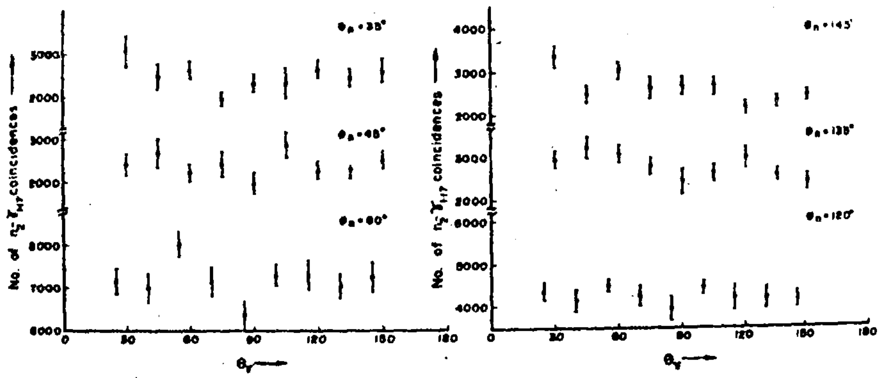

FIG. 18

It is hoped that a clearer picture of the reaction mechanism might emerge when the analysis of the entire data is completed. It might then be possible to extract information about the multipole nature of the gamma radiations involved in $n - \gamma$ correlations from a comparison of the experimental results with theoretically calculated values.

References:

1) G.R. Satchler, Phys. Rev. 94 (1954) 1304 and 104 (1956) 1198.

2) G.S. Mani, M.A.Melkanoff and I.Iori, Proton penetrabilities using an optical model potential - Rapport C.E.A. N°. 2379, Saclay, 1963.

3) G.S.Mani, M.A. Melkanoff and I.Iori, Neutron penetrabilities using an optical model potential - Rapport C.E.A. N°. 2380, Saclay, 1963.

4) A.T. G. Ferguson and G.C.Morvison, Proceedings of the International Conference on the neutron interactions with nucleus, Columbia University, New York, 9 - 13, 1957, TID 7547.

5) E. Sheldon, Rev. Mod. Phys. 35 (1963) 795

6. Measurement of the integrated cross sections of (α, n) and (p,n) reactions - K.K. Sekharan, A.S.Divatia, M.K. Mehta and S.S.Kerekatte - The integrated cross section of $^{51}V(p, n)^{51}Cr$ reaction has been determined for the incident proton energy range of 2.8 to 5.5 MeV using a 45 KeV thick vanadium target for 3 MeV protons. Neutrons were detected by a calibrated 4π counter consisting of a BF_3 counters-paraffin assembly. To evaluate the cross section for the incident proton energy range of 1.9 to 2.8 MeV the neutron yield from a thin vanadium target was averaged and normalized with the 45 KeV thick target yield. The cross section is shown in Fig. 19 as a function of the incident proton energy.

The target was prepared by evaporation of vanadium on to a weighed aluminium foil. The target was mounted on a rotatable target holder with a thick piece of tantalum as backing. The background was measured by turning the target through 180°. The background was only 2% at low incident energies but was 5% at 5.5 MeV.

The coulomb barrier for the vanadium nucleus is nearly 5 MeV. From the exponential rise of the cross section value, it is evident that the cross section at low incident energies is influenced by the coulomb barrier. As the incident energy increases the number of levels which are simultaneously excited will be more since the level density increases. The rapid increase in the cross section observed in the present measurement is likely to be due to the combined effect of overcoming the coulomb barrier and an increase in the level density.

The reaction which contributes mainly to the total cross section of protons on vanadium is the (p, n) reaction. The other energetically possible reactions are the proton inelastic scattering, (p, γ) and (p, α) reactions. The cross sections for (p, γ) and (p, α) reactions are expected to be less than 10 mb. in this energy range. The (p, p') cross section is found to be approximately 25 mb at 5 MeV. Therefore, all these reaction cross sections added together form only a fraction of the total cross section. Thus, if the (p, n) cross section is determined accurately the total reaction cross section can be obtained and this enables one to compare the experimental values with those calculated on the basis of the optical model.

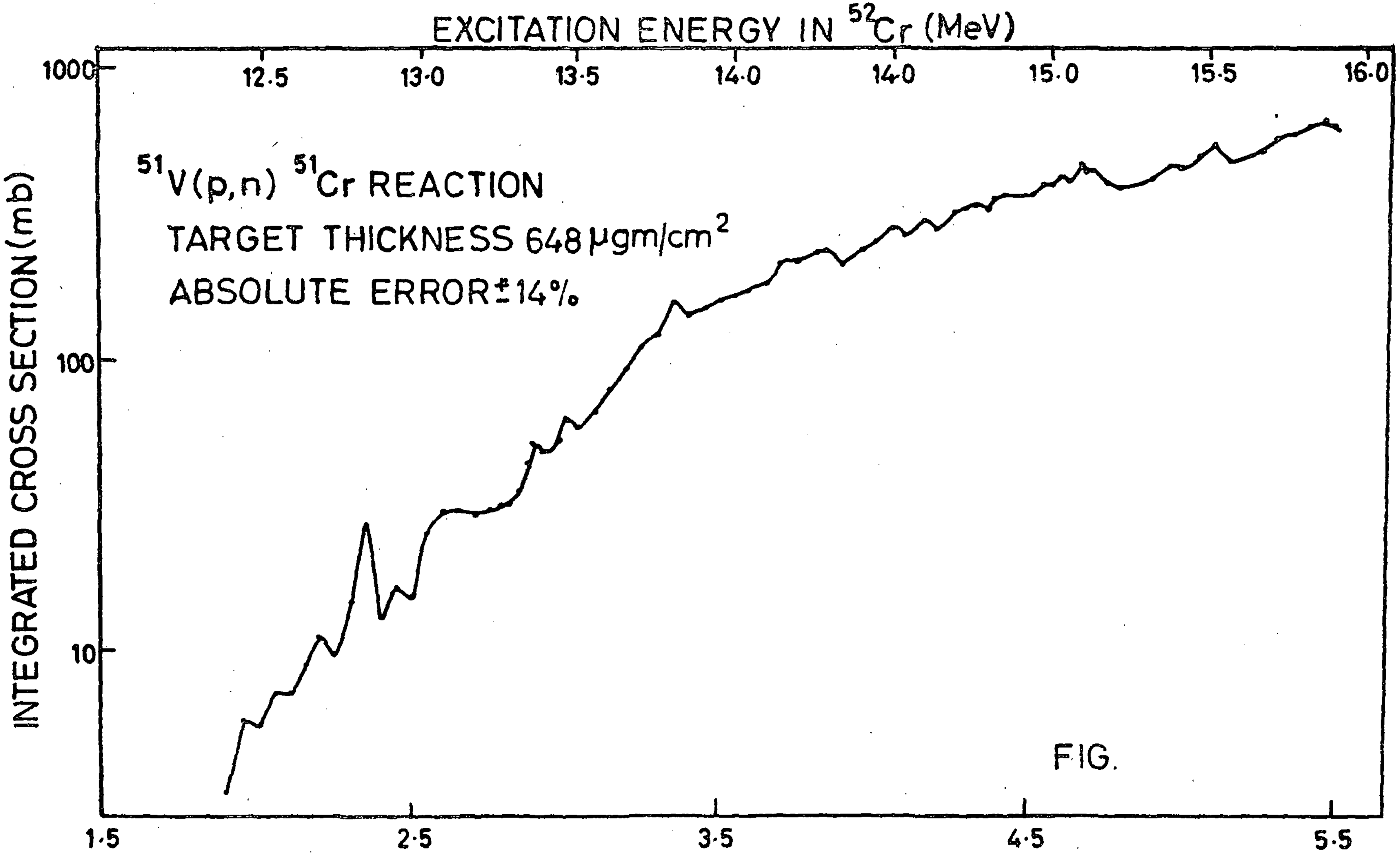

FIG.19. ENERGY PROTONS (MeV)

The experimental details of the $^{13}C(\alpha, n)^{16}O$ reaction[1] which was measured for the incident alpha particle energy range of 1.95 MeV to 5.5 MeV and the $^{19}F(\alpha, n)^{22}Na$ reaction[2] which was measured from 2.5 to 5.5 MeV have been explained previously. The integrated cross section of the $^{19}F(\alpha, n)^{22}Na$ reaction shows more than 30 resonances in the incident alpha particle energy range of 2.5 to 5.5 MeV corresponding to the excitation energy range of 12.5 to 15 MeV in the compound nucleus ^{23}Na indicating many levels in ^{23}Na. The $^{13}C(\alpha, n)^{16}O$ reaction cross section shows 20 resonances in the excitation energy range 7.8 to 10.5 MeV of the compound nucleus ^{17}O. Many of the resonances observed are well isolated and hence the Breit Wigner single level dispersion theory has been applied to obtain the values of the level parameters. The Breit Wigner single level formula is of the form

$$\sigma(\alpha, n) = \pi \lambda_{\alpha}^{2} \frac{(2J+1)}{(2I+1)(2i+1)} \frac{\Gamma_{\alpha} \Gamma_{n}}{(E-E_R)^2 + \left(\frac{\Gamma}{2}\right)^2}$$

The values of J and Γ are known for the levels in ^{17}O. The product $\Gamma_{\alpha} \Gamma_{n}$ of the partial widths was calculated for six resonances assuming the values of J and Γ. The values of Γ_{α} and Γ_{n} were calculated by assuming that $\Gamma_{\alpha} + \Gamma_{n} = \Gamma$ and $\Gamma_{n} > \Gamma_{\alpha}$. These values are tabulated below.

Using the reciprocity theorem the integrated cross section of $^{16}O(n, \alpha)^{13}C$ reaction was determined for the alpha particle energy range upto 5.05 MeV. This is the threshold value for the reaction $^{13}C(\alpha, n)^{16}O$ leaving ^{16}O in the first excited state. Therefore, the cross section of (n, α) reaction cannot be calculated beyond this energy.

TABLE

E_α MeV	$\Gamma_\alpha \Gamma_n$ (KeV)^2	Γ_α (KeV)	Γ_n (KeV)
2.70	4.60	0.62	7.38
2.82	7.38	1.73	4.27
3.73	0.84	0.22	3.78
4.13	3.86	0.36	10.64
4.44	53.74	3.46	15.54
4.63	15.92	1.52	10.48

References:

1) Study of the integrated cross sections of (p, n) and (α, n) reactions. M.Sc. Thesis by K.K.Sekharan, University of Bombay, 1965.

2) K.K.Sekharan, M.K. Mehta and A.S.Divatia, Proceedings of the Nuclear Physics and Solid State Physics Symposium, Nuclear Physics, Department of Atomic Energy, Government of India (1965) 199.

7. Elastic scattering of alpha particles by ^{24}Mg - S.S.Kerekatte, M.K. Mehta, A.S.Divatia and K.K.Sekharan - Elastic scattering of alpha particles from ^{24}Mg has been observed at 80.5° and 164°. The incident alpha particle energy was varied from 3.440 to 5.500 MeV, in steps of 5 to 10 keV. The corresponding excitation energies in the compound nucleus ^{28}Si, are from 12.935 to 14.700 MeV. The target consisted of ^{24}Mg isotope deposited on carbon backings of 10 ug/cm^2. The thickness

of the target was found to be 25 KeV for 1.37 MeV alphas. Since, carbon and oxygen cross sections are known, the thickness of ^{24}Mg can be determined.

The excitation function at 164° (Fig. 20) shows ten resonances at 3.520, 3.600, 3.825, 4.580, 4.640, 4.870, 5.125, 5.135, 5.200 and 5.415 MeV. These correspond to levels in ^{28}Si. They are superposed on a fairly smooth curve which is probably due to Rutherford scattering.

8. Three body break up reactions - A.S.Divatia, M.K.Mehta and S.S. Kerekatte - The roles played by two body and three body forces can be investigated by a study of three body break up reactions. A preliminary study of such reactions has been undertaken; experimental equipment is being designed.

9. Energy levels of ^{27}Al - A.S.Divatia, M.K.Mehta and S.S.Kerekatte - Energy levels in ^{27}Al at 0.84, 1.01, 2.21, 2.73, 2.98 and 3.00 MeV are well known. Some workers[1, 2] have reported experimental evidence regarding the existence of two more levels in this region, at 1.65 and 1.83 MeV. Since the existence of these two levels would make a significant difference in the nuclear structure calculations for the ^{27}Al nucleus, a careful search for the two levels was undertaken when a study of p + ^{27}Al reactions was being done. The aluminium targets, made from specpure aluminium metal, were bombarded by 3.5 - 5.5 MeV protons. The charged particle reaction products comprised the elastic proton group, the inelastic proton groups corresponding to the levels at 0.84, 1.01, 2.21 and 2.73 MeV, and the alpha groups from the

$^{27}Al(p,\alpha_0)^{24}Mg$ reaction. A weak but definite charged particle group was observed between the groups corresponding to the levels at 1.01 and 2.21 MeV. On the basis of its energies at various angles, the group appeared to be an inelastic proton group corresponding to a level in ^{27}Al at 1.75 MeV. However, by observing the yield of this group for different ^{27}Al targets, and by obtaining an excitation curve, it could be established that the group was not due to the $^{27}Al(p,p_{1.78})^{2'}$ reaction but due to the $^{28}Si(p, p_{1.78})^{28}Si^*$ reaction. The silicon conte in the aluminium used was determined to be about 50 ppm, by spectroscopi analysis. Since this low a fraction could not explain the yields observed, it was felt that the silicon was deposited as a contamination on the target due to the silicon vacuum grease used in the systems. It is concluded that the proton excitation cross section for the 1.65 and 1.83 MeV levels in ^{27}Al is less than 0.4 mb/sr, for incident proton energies upto 5.5 MeV.

References:

1) L. Ciufolotti and M. Demichelis, Nuclear Phys. 39 (1962) 252.

2) S.S.Vasilev et al., Sov. Phys. JETP 20 (1965) 1064.

10. X-ray yields from K.shell ionization by α-particles* - R.P.Sharma[@] B.V.Thosar[@] and K.G. Prasad[@] - The characteristic K X-ray yields are measured in Sn, Te, Cc, ^{144}Sm, ^{152}Sm, ^{154}Sm, ^{160}Gd, ^{186}W and P_b by bombarding them with α particles of energy 4 and 3 MeV. No excess of X-ray yield has been observed in the atoms of deformed

---

@ Tata Institute of Fundamental Research, Bombay.

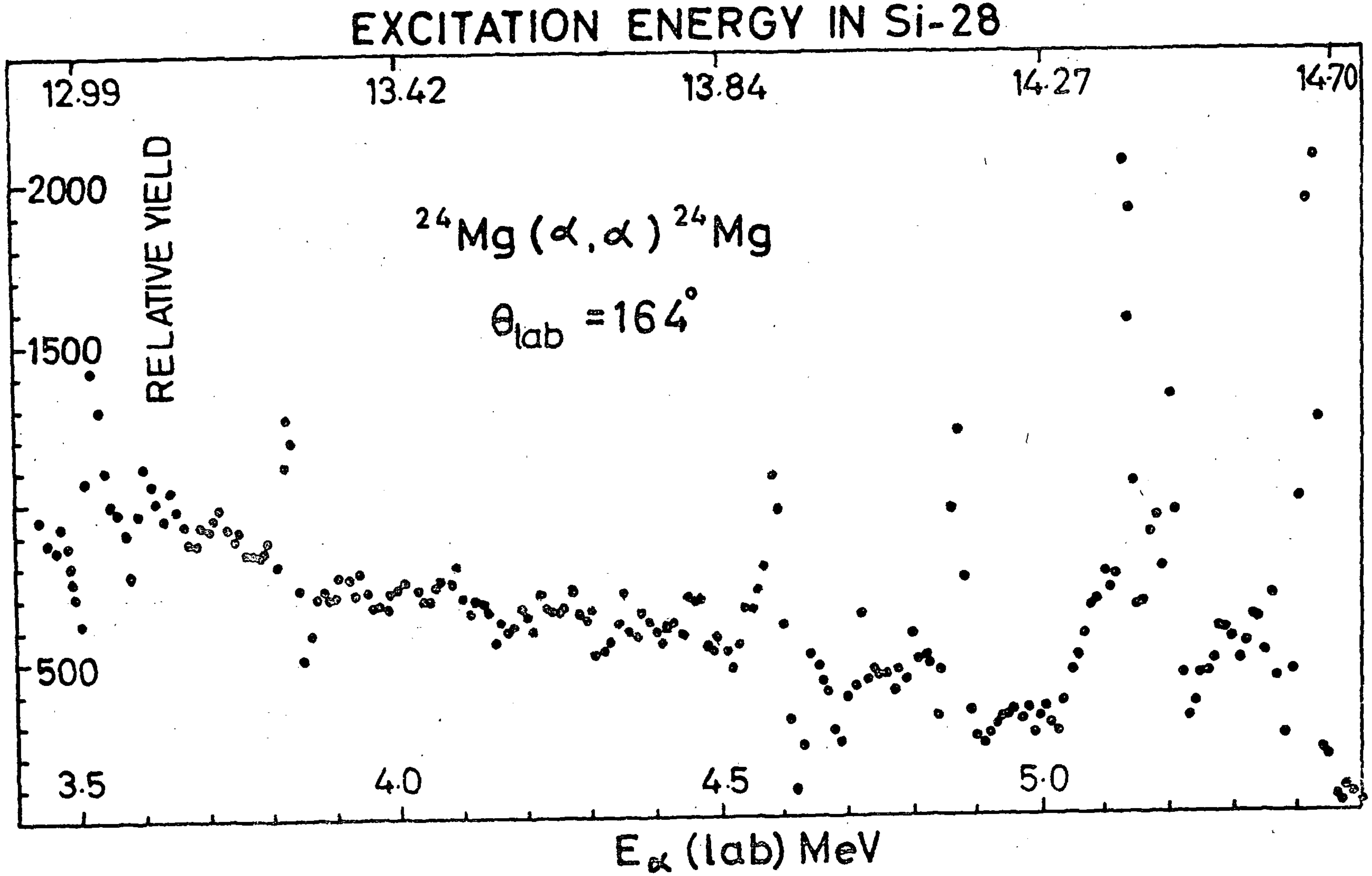
EXCITATION ENERGY IN Si-28
12.99
13.42
13.84
14.27
14.70
RELATIVE YIELD
2000
1500
500
$^{24}Mg(\alpha,\alpha)^{24}Mg$
$\theta_{lab} = 164°$
3.5
4.0
4.5
5.0
E_α (lab) MeV

FIG. 20.

even-even nucleii, when the observed data were corrected for X-ray contribution due to internal conversion by using the theoretical values of K shell internal-conversion coefficients. The observed variation of the number of K-shell vacancies per micro-coulomb with the atomic number indicates that the E2 internal-conversion coefficients and also the probability for K-shell ionization are unaffected by nuclear deformation.

* Published in Phys. Rev. 140, 4A (1965) 1084.

11. Angular distribution of the $^{19}F(n,\alpha)^{16}N$ reaction at $E_n = 4.7$ MeV - S.M. Bharathi[@], U.T. Raheja[@] and E. Kondaiah[@] - The study of energy and angular distribution of alpha particles arising from the $^{19}F(n,\alpha)^{16}N$ reaction at $E_n = 4.7$ MeV was continued in Van de Graaff, in order to supplement the data obtained in 1963. A gas proportional counter telescope[1] was used for this study. A titanium-tritium target bombarded with 5.5 MeV protons from the Van de Graaff Accelerator served as the source of neutrons. The angular distribution fits well with a Legendre Polynomial $a_0 + a_1 P_1 (\cos\theta)$ with $a_0 = 1.0 \pm 0.1$ and $a_1 = 0.4 \pm 0.15$, showing interference between resonances occurring in the neighbourhood of $E_n = 4.7$ MeV used in this study. The cross section for this reaction is obtained as 175 ± 18 mb by comparing the yield of this reaction at 0° with the yield of recoil protons from an alkathene target. The measured cross section agrees within limits of error with the cross section 150 ± 40% mb reported by Marion and Brugger[2]. This paper is under publication in 'Nuclear Physics'.

@ Tata Institute of Fundamental Research, Bombay.

References:

1) T.P. David, Van de Graaff Laboratory Progress Report, AEET-214 (1965) 31.

2) J.B. Marion and R.M. Brugger, Phys. Rev. 100 (1955) 69.

12. Proton induced reactions in Vanadium - C.M. Lamba, N. Sarma, V.K. Deshpande[@], G.K.Mehta[@] and D.K.Sood[@] - Recent high resolution experiment have brought to light the existence of rapid fluctuations in excitation functions. These wide ($\sim$ 150 KeV) fluctuations occur at excitation energies of about 25 KeV in the compund nucleus. At such energies it was expected that $\Gamma \gg D$ and the excitation functions would be smooth. Direct mechanism is also expected to give rise to smooth excitation functions. The observed fluctuations were accounted for by Ericson aft re-examination of the conventional statistical theory. He further prescribed techniques of obtaining information about average level width and the percentage of direct reaction contribution from the observed fluctuations. Further, outstanding resonances have been observed in th continuum region recently and they have been interpreted as levels of simple configurations of the compound nucleus. From these points of view it was of interest to make a high resolution study of the excitatio function.

Vanadium-51 was chosen as the target material. The Van de Graaff accelerator was used to obtain proton beam of intensity of about .25 microamperes in the energy range 2.5 to 5.5 MeV with an expected

---

@ Indian Institute of Technology, Kanpur.

beam energy resolution of less than 5 KeV. The beam energy was changed in 5 KeV steps. Vanadium targets were made by evaporating metallic vanadium of thickness a few KeV on carbon backings. Surface barrier solid state detectors with resolution of about 25 KeV were employed. A four hundred channel analyser (used as four 100 channel analysers) in conjunction with low-noise charge sensitive amplifying systems was used to analyse the detector outputs. The detectors had to be placed at angles beyond 80 degrees to resolve the various peaks.

Analysis of data:

The measurement of excitation functions in using a Van de Graaff Accelerator is an extremely tedius process and involves several months of analysis of data accumulated in a week. A full excitation function from 2.5 to 5.5 MeV at 5 KeV intervals implies 600 measurements, i.e. 600 x 400 i.e. about quarter million numbers, and thus presents an ideal case for computer processing. A method was therefore developed to analyse the data by using the computer CDC-160A and CDC-3600.

In this scheme, the output of the analyser was punched on a 8 level binary coded decimal paper tape. The run number and clock time are punched manually on the tape between certain code symbols prior to data. Each analyser output number is of 9 digits, the first three being the address the next six the accumulated counts. The run number and clock time are of 3 and 6 digits respectively. The first channel output indicates the live time of analyser.

A programme has been written in machine language to transfer the data on magnetic tape and to get a print output of the raw data. The computer CDC-160A is used for this purpose. Several checks and error correcting procedures have been built in to take account of errors in punch output.

A second programme on punched cards giving the relation between run number and incident energy, the masses and Q.values for each reaction, the angle of observation of each detector and the calibration data of particle energy versus channel number for each detector is fed to the CDC-3600 to analyse the data. Using the method of least squares linear fits for the calibration of all the 4 detectors were obtained.

The above programme calculates the output energy and from the calibration data the channel number at which each peak is expected. It then looks for the peak using following criteria.

1. A peak in any channel is defined when the counts in that channel are more than those on either side.
2. If a peak is not found in the expected channel, it searches N channels on both sides where N is preset.
3. If there are two peaks in this region, the peak nearest to expected channel is chosen.
4. If no peak is observed or when two peaks are observed equally spaced from where it is expected, the fact is printed.

The following criteria are used to find the area under the peak:

1. The peak is defined to be between the two prints where the slope curve is zero.
2. The background is defined to be linear between those two points.
3. The counts under the peak are summed and the background as defined is subtracted.
4. The counts under the peak are corrected for the dead time of analyser using the formula:

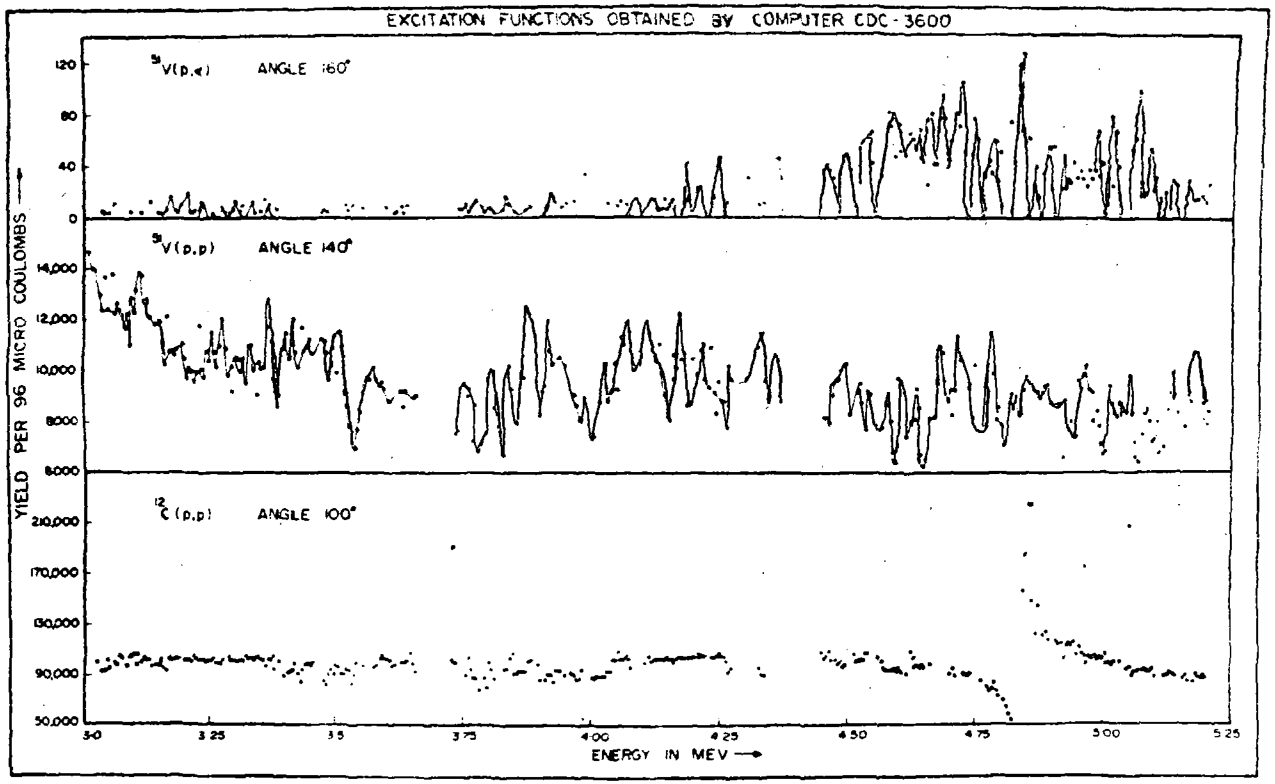
EXCITATION FUNCTIONS OBTAINED BY COMPUTER CDC-3600
51V(p,α) ANGLE 160°
51V(p,p) ANGLE 140°
12C(p,p) ANGLE 100°
YIELD PER 96 MICRO COULOMBS
ENERGY IN MEV
120
80
40
0
14,000
12,000
10,000
8000
6000
210,000
170,000
130,000
90,000
50,000
3.0
3.25
3.5
3.75
4.00
4.25
4.50
4.75
5.00
5.25

FIG. 21.

$$\text{Corrected area} = \frac{\text{Clock time}}{\text{Live time}} \times \text{uncorrected area}$$

The use of this method can be seen by looking at following figures. Data measured on a previous occasion for one group, two angles and 270 energies took seven months for an incomplete analysis. Data analysed by computer for 4 angles and 440 energies involved 15 minutes of CDC-3600 time, about 8 hours to load the paper tape and 16 hours to plot the excitation functions.

Minor modifications have been made to use this programme to evaluate angular distribution and angular correlation data.

Results:

Excitation functions for the reactions $^{51}V(P, P)$, $^{12}C(P,P)$ $^{16}O(P, P)$ and $^{51}V(P, \alpha)$ were measured at three angles 100, 140, 160°. The results indicated the presence of very strong fluctuations in the excitation function. A comparison with a previously measured excitation function for ^{12}C showed that the results were reliable. Fig. 21 shows some of the excitation functions obtained. Statistical analysis of the data in terms of autocorrelation and cross correlation functions are in progress.

INSTRUMENTATION AND DATA PROCESSING

1. A two parameter analysing facility for coincidence experiments in Nuclear Reactions - N.L. Ragoovansi, P.C. Mitra and M.A. Eswaran - For use in coincidence experiments in Nuclear reactions involving simultaneous pulse height analysis of spectra from two different radiation detectors, a system has been built which extends the utility of the TMC 400 channel pulse height analyser to that of a two parameter analyser by making use of a 20 channel Gatti type pulse-height analyser. This is facilitated by incorporating fast-slow coincidence systems.

The outputs from the two detectors are fed to a fast coincider circuit after proper fast amplification. The output linear pulses from one of the detectors are analysed in the 20 channel pulse height analyse from which any desired spectrum region can be selected to give a gating signal to a slow coincidence circuit which is fed by the fast coincidenc output. The output linear pulses from the second detector are analysed in one quarter of the TMC 400 channel analyser gated by the output of the fast-slow coincidence assembly. For such coincidence spectra in the four quadrants of the TMC 400 channel analyser can be recorded, each one being gated by the output signal from four slow coincidence assemblies, each of which is fed by pulse from a selection window set on the first detector spectrum analysed in the 20 channel analyser.

The fast coincidence circuit resolving time is variable in the range 2τ = 40 - 200 nanoseconds. An additional feature incorporated in this assembly is the use of the two similar fast coincidence units of same resolving time but with a large delay of 1 microsecond, introduced in one of the fast input channels in the

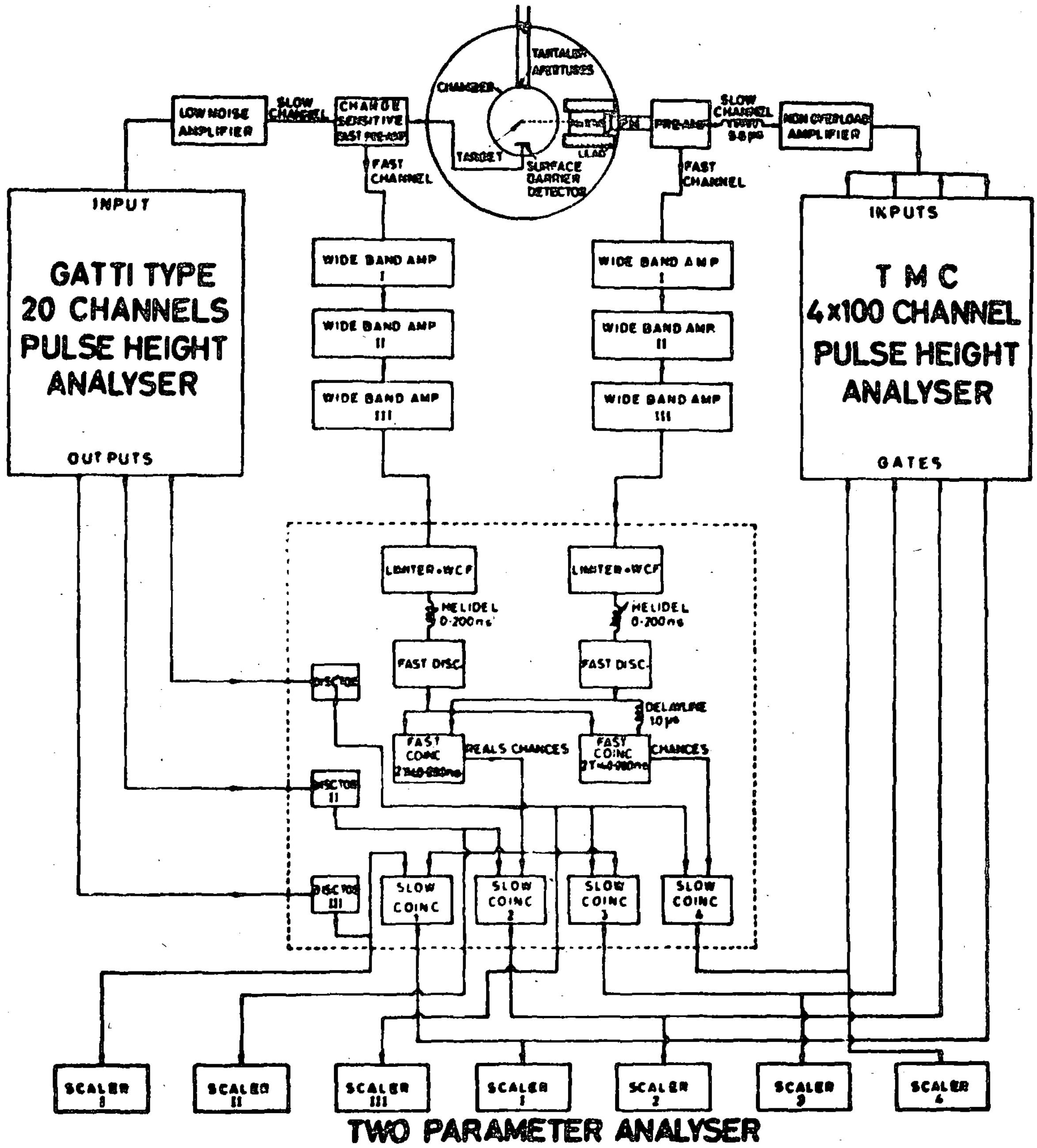
TANTALUM APERTURES
CHAMBER
TARGET
SURFACE BARRIER DETECTOR
LEAD
LOW NOISE AMPLIFIER
SLOW CHANNEL
CHARGE SENSITIVE FAST PRE-AMP
FAST CHANNEL
PRE-AMP
SLOW CHANNEL
NON OVERLOAD AMPLIFIER
INPUT
GATTI TYPE 20 CHANNELS PULSE HEIGHT ANALYSER
OUTPUTS
INPUTS
T M C 4x100 CHANNEL PULSE HEIGHT ANALYSER
GATES
WIDE BAND AMP I
WIDE BAND AMP II
WIDE BAND AMP III
LIMITER+WCF
HELIDEL 0-200 ns
FAST DISC
DELAY LINE 1.0 μs
FAST COINC
REALS
CHANCES
DISCTOR I
DISCTOR II
DISCTOR III
SLOW COINC 1
SLOW COINC 2
SLOW COINC 3
SLOW COINC 4
SCALER I
SCALER II
SCALER III
SCALER 1
SCALER 2
SCALER 3
SCALER 4
TWO PARAMETER ANALYSER

FIG. 22.

second fast coincidence unit. Hence the output of this second fast coincidence unit correspond to random coincidences. Using this, random coincidence spectrum can be recorded in one quadrant of TMC 400 channel analyser simultaneously with the true plus random spectrum thereby increasing the reliability of the data in the nuclear reaction experiments where the source strength is liable for large fluctuations due to the changes in the beam intensity on the target. The essential features of this two parameter analysing facility is shown in the block diagram in Fig. 22. This facility has been made use in proton-gamma ray angular correlation measurements in the reaction $^{26}Mg(d, p\gamma)^{27}Mg$.

2. <u>Design and performance of a getter-ion pump</u>* - K.B. Nambiar and A.S.Divatia - A getter-ion pump in which titanium is evaporated by electron bombardment has been built and its performance when connected to a metal system has been tested. The lowest pressure achieved by this pump is $\sim 2 \times 10^{-7}$ mm of Hg. Its pumping speed is comparable to that of a 2 in mercury diffusion pump.

* Published in the Ind. J. of Pure and Appl. Phys. 3, 7 (1965) 271.

3. <u>Split-pole magnetic spectrograph</u> - M.N. Viswesvariah and N. Sarma - A design study of the charged particle magnetic spectrographs was undertaken and several types of instruments were studied. These included the Browne-Buechner type[1] and Elbek type[2] of instruments which give focusing of second order over part of the entire momentum range.

Detailed study of the split-pole type of magnetic spectrograph was (Fig. 23) carried out. Equations were derived for the locus of focii for different momenta, the variation of energy resolution, dispersion and lateral magnification. One important feature of the SPMS is the focusing it produces for charged particles in the vertical plane giving rise to better values of the signal to noise ratios at the final image. The split-pole type of spectrograph consists of a circular sector magnet with circular pole boundaries and a straight sector magnet with straight pole boundaries. The circular sector produces virtual images of the source. The locus of these images including the source is approximately a circle whose radius has a value between the entrance and exit radii of curvature for the circular sector. The second magnet produces real images of these virtual sources very nearly along a plane surface.

The variation of the lateral magnification, energy resolution and dispersion are shown in Fig. 24 for charged particle orbits of different radii in the magnetic fields of the two sectors.

References:

1) C.P. Browne and W.W. Buechner, Rev. Sci. Instr. 27 (1965) 899.
2) J. Borggreen, B. Elbek et al. Nucl. Instr. Meth. 24 (1963) 1.

4. A circuit for preventing accumulation of experimental data when the nuclear reaction rate exceeds a preset value - S.K. Gupta[@], K.V.K. Iyengar[@] and P.J. Bhalerao - A circuit has been devised to restrict accumulation of (n,γ) angular correlation data in $A(x, n\gamma)B$ type

---

@ Tata Institute of Fundamental Research, Bombay.

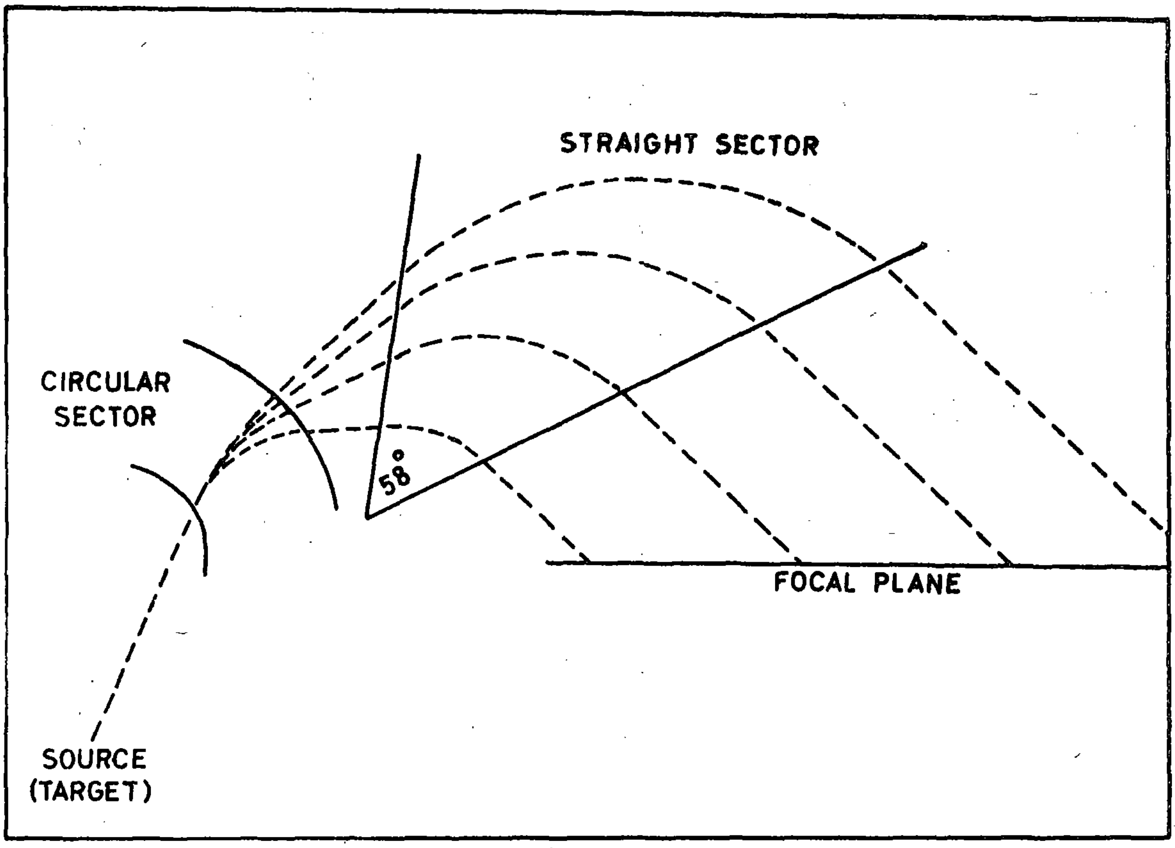
STRAIGHT SECTOR
CIRCULAR
SECTOR
58°
FOCAL PLANE
SOURCE
(TARGET)

FIG. 23.

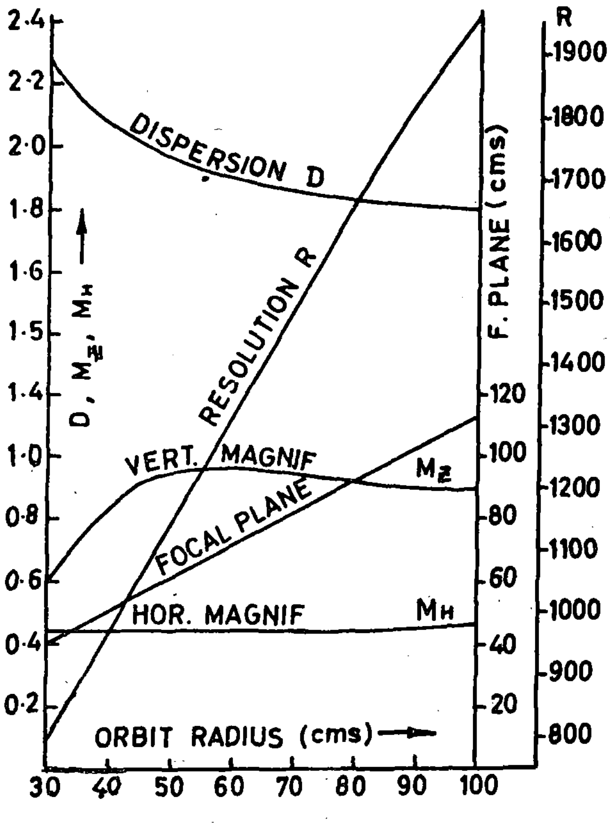
2.4
2.2
2.0
1.8
1.6
1.5
1.4
1.0
0.8
0.6
0.4
0.2
D, M_z, M_H
DISPERSION D
RESOLUTION R
VERT. MAGNIF
M_z
FOCAL PLANE
HOR. MAGNIF
M_H
ORBIT RADIUS (cms)
30 40 50 60 70 80 90 100
F. PLANE (cms)
120
100
80
60
40
20
R
1900
1800
1700
1600
1500
1400
1300
1200
1100
1000
900
800

FIG. 24.

reactions only to periods when the counting rate in the gamma detector is below the fatigue level of the photomultiplier and its gain insensitive to changes in the counting rate.

5. <u>Computer programmes for fluctuation analysis</u> - M.K. Mehta - When a nuclear reaction proceeds through the formation of a compound nucleus of high excitation energies, the excitation curve exhibits structure which looks like resonances, but in fact is due to statistical fluctuation in an otherwise smooth curve which would be expected if the ratio Γ/D - the average level width to average level spacing in the compound nucleus is greater than unity. The data in such cases are examined in terms of two correlation functions which are defined as follows:

$$C(\epsilon) = \frac{\Delta E}{E_2 - E_1} \sum_{E=E_1}^{E_2} \left(\frac{\sigma E}{\langle \sigma E \rangle} - 1\right)\left(\frac{\sigma(E+E)}{\langle \sigma(E+E) \rangle} - 1\right)$$

where $C(\epsilon)$ is the autocorrelation function, E_1 and E_2 are the lowest and the highest energies in the excitation curve. ΔE is the experimental energy interval between two successive data points and $E = n\,\Delta E$ where n is an integer

$$C_{ab}(\epsilon) = \frac{\Delta E}{E_2 - E_1} \sum_{E=E_1}^{E_2} \left(\frac{\sigma_a(E)}{\langle \sigma_a(E) \rangle} - 1\right)\left(\frac{\sigma_b(E+E)}{\langle \sigma_b(E+E) \rangle} - 1\right)\frac{1}{C_a(0)\,C_b(0)}$$

where $C_{ab}(\epsilon)$ is called the cross correlation between curves a and b and $C_a(0)$ and $C_b(0)$ are the autocorrelations for the curves a and b respectively for $E = 0$; the other quantities are already defined. Typical excitation curves have as many as 300 points, thus for every ϵ these expressions involve summing over 300 quantities and there could be as many as 300 values for ϵ . Thus such calculations can be carried out only by means of a fast digital computer.

All this is to be done for a particular averaging interval δ which is involved with averages $<\ >$ appearing in the denomenators. It was proposed to vary this energy interval δ and calculat the correlations as a function of this δ to bring out if possible any underlying structure which may be due to genuine resonances.

Two computer programmes have been written in Fortran language to be used on the CDC-3600 computer at T.I.F.R. to do the above mentioned calculation. Programme No. 1 calculates the auto and cross correlations for as many as five curves each having 300 experimental points for a range of energy intervals that have to be read in. The input consists of the uppermost and the lower most energies, number of excitation curves, number of points in each curve, number of energy intervals to be used, and the energy interval δ themselves. This is followed by the actual data in terms of relative yields or absolute cross sections. The second programme first takes the full energy range and divides it into smaller sections, the range of each to be read in. It then calculates the auto and cross correlations for each of these section separately using an averaging interval which is equal to the full range of each particular section. In this case the input consists of the number of curves, number of data points on each curve, the lowest and highest energies and the number of sections. This is followed by the lower and the upper energies for each section, and the actual data in terms of relative yields or absolute cross sections.

Both of these programmes have already been used in the analysis of the ^{27}Al and p experiments and have produced very significant results. A number of experiments are now being planned by the charge particle reactions section with a view to obtain knowledge about level densities at excitations between 10 and 20 MeV in compound nuclei having masses between mass numbers 25 and 30. These computer programmes will be extensively used for the analysis of the results of these experiments.

6. Carbon films - S.S. Kerekatte, K.K. Sekharan and K.B. Nambiar - Carbon films of 10 $\mu g/cm^2$ have been made in this laboratory. Carbon was evaporated on to glass slides having an NaCl layer. The evaporation was done by striking an arc between two carbon electrodes whose motion could be controlled from outside. The films were floated off in water and picked up on holders. The thickness was determined by measuring the energy loss of alpha particles in passing through the film. It was found to be 16 KeV for 1.37 MeV alphas, which corresponds to 10 $\mu g/cm^2$. These films have been used as backings in several experiments.

7. The efficiency of a getter-ion pump - K.B. Nambiar and A.S.Divatia - Investigations have been made to study the efficiency of a getter-ion pump[1)]. Factors like outgassing of the system and the performance of the getter material strongly influence the efficiency of the pump.

The rate of outgassing of the system before and after prolonged baking have been obtained by recording the pressure in the system at regular intervals after the 'shut-off'. Pressure vs. time curves are plotted (Fig. 25). From a comparison of the curves it is seen that in a non-baked system, within a few minutes after the 'shut-off' the pressure recorded is about 100 times higher than that recorded in a baked system. From a typical 'residual' rate of rise[2] - that is, the lowest rate of pressure rise attainable - it was seen that after the first few minutes, the rate of pressure rise is approximately 5×10^{-13} mm Hg/sec., whereas it is $\sim 6 \times 10^{-9}$ mm Hg/sec. in the system dealt with in this laboratory.

Different materials were tried out in the pump as getter, in order to study the effective role played by titanium in this pump. The materials were tested separately as anodes in place of titanium. In the case of aluminium an ultimate vacuum of $\sim 2 \times 10^{-6}$ mm of Hg was achieved and was being maintained in the system. Speeds for air ranging from 1.5 to 3.5 litres/sec. were obtained at $p = 2 \times 10^{-4}$ mm of Hg. The pumping speed for hydrogen was found to be negligible. Though aluminium readily forms compounds with active gases like oxygen and nitrogen its gettering efficiency is low. Barium, an alkaline earth metal and known to be a good getter, was tried out in the pump and an ultimate vacuum of 2×10^{-6} mm of Hg was attained. A pumping curve with barium used as getter is shown in Fig. 26. The pumping speed estimated was of the order of 0.5 litre/sec. with little quantities of barium being evaporated at a time. The metal has a high affinity for oxygen and hydrogen. One disadvantage with alkaline earth metals is that their films flake off at very early stages of their formation. This is one of the reasons why barium is not suitable for such pumps where the metal is continuously evaporated. Besides, barium and its compounds have high vapour pressures. Copper, though evaporated in large quantities, failed to establish any pumping action. Though

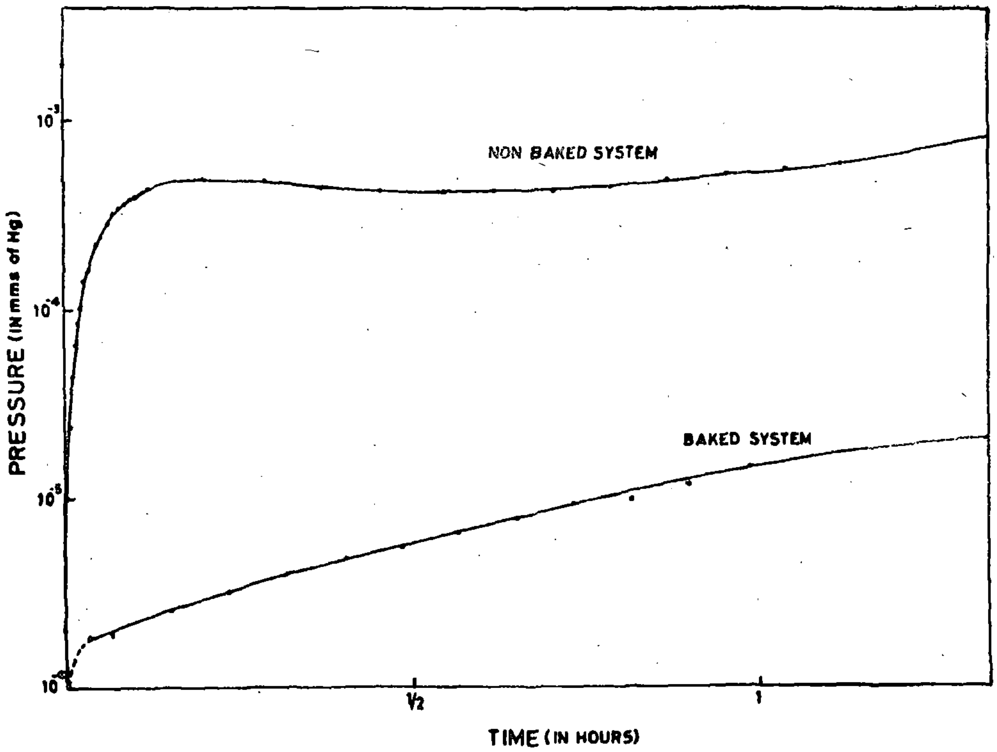
NON BAKED SYSTEM
BAKED SYSTEM
PRESSURE (IN mms of Hg)
10⁻³
10⁻⁴
10⁻⁵
½
1
TIME (IN HOURS)

FIG. 25.

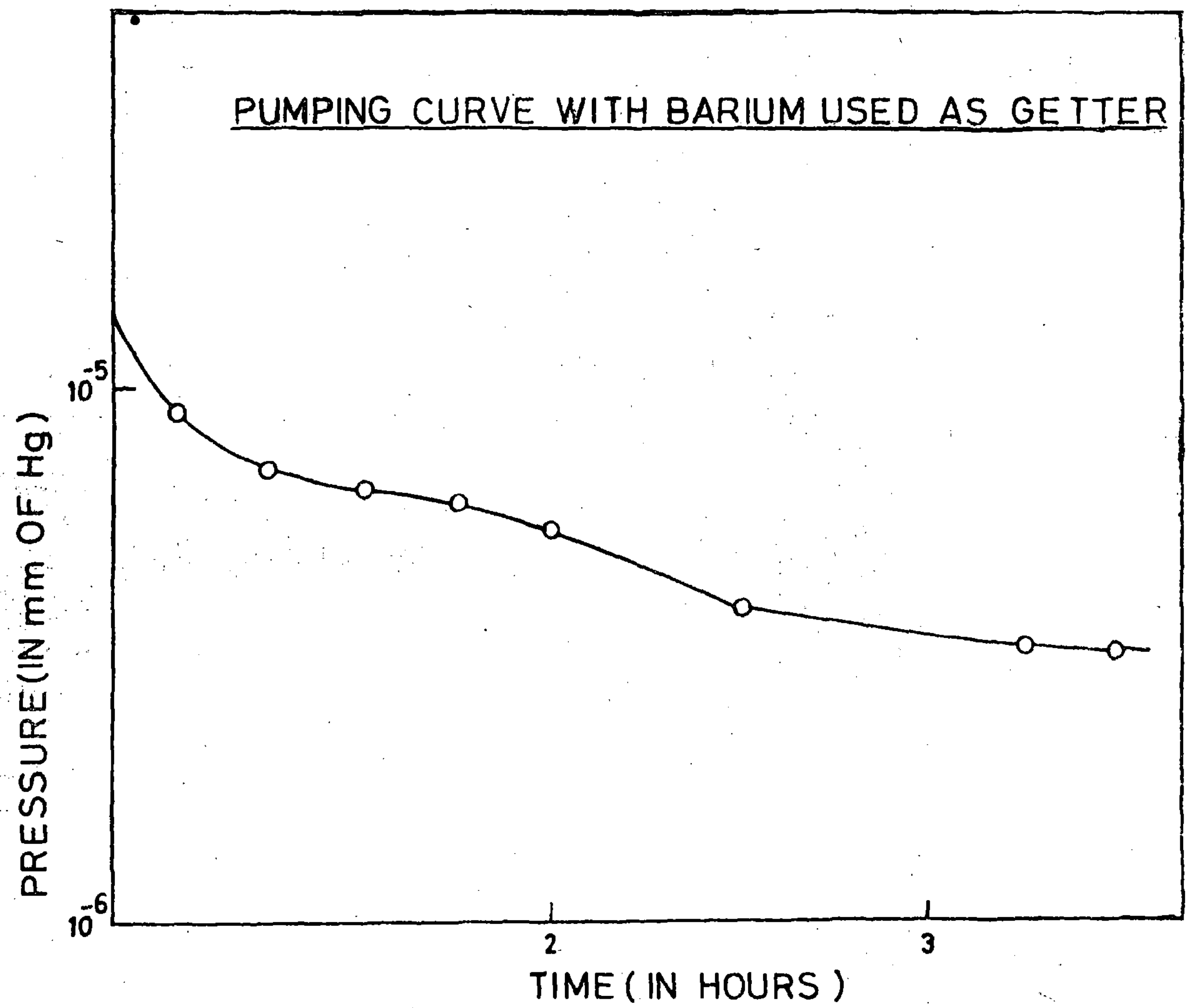
PUMPING CURVE WITH BARIUM USED AS GETTER
PRESSURE (IN mm OF Hg)
10⁻⁵
10⁻⁶
2
3
TIME (IN HOURS)

FIG. 26.

the vapour pressure is not high in this case, the metal does not possess the properties of a getter.

Of all the metals, titanium is one of the most efficient getters. The metal and its compounds are quite stable at room temperature; its vapour pressure at high temperatures is so low that it does not come in the way of attaining very high vacua.

References:

1) K.B. Nambiar and A.S.Divatia, Indian J. Pure & Appl. Phys. 3, 7 (1965) 271.

2) D. Alpert, Handbuch Der Physick, XII (1958) 661.

8. Current integrator - M. Bhatia, N.S. Thampi and N. Sarma - A reliable current integrator has been built at the Van de Graaff Laboratory for use with small currents. The design is based on a paper of H.A.Enge[1]. It is of the input capacity type, in which the condenser is charged by the input current to a certain voltage and then discharged quickly by an electronic device.

Fig. 27 is a circuit diagram of the complete integrator, vacuum tube voltmeter and register drive circuit. C_1 is the integrating condenser, whose value is dependent upon the magnitude of the current to be integrated. The double triode V_1V_2 is connected in a univibrator circuit. Normally V_2 is conducting since the voltage on its grid is kept at about 30 - 35 volts by adjusting R_{10}. The cathode voltage is subsequently slightly higher. The grid voltage of V_1 rises as condenser C is charged by the input current. When the grid reaches 35 volts, V_1 starts conducting. This causes the univibrator to flip over causing V_2 to be cut off. The relay Re_1 operates and discharges C_1

through its contact a and resistance R_1. The univibrator again flips back and V_1 is cut off . Due to mechanical and electrical inertia the relay remains energised for about 2 ms, which is sufficient time for discharging C_1.

The charge collected depends upon the value of C_1. For C_1 = .005 u F, the charge collected per cycle of operation = 35 V x .005 u F = 0.175 u C.

The contact b of relay Re_1 completes the circuit for a preset counter.

The vacuum tube voltmeter comprises of a double triode V_3 V_4 which is connected as a balanced D.C. Amplifier. A 50 uA meter is connected as shown in the circuit. The switch SW_1 selects the appropriate shunt resistance from the combination R_3, R_4, R_5 for indication of the input current.

The voltage drop across the shunt resistors also compensates for the error of integration caused by the inertia of the flipping circuit and relay. The effect is explained below. When grid of V_1 reaches voltage E, the circuit starts to flip over. Irrespective of the input current, it now takes time Δt to operate the relay, to discharge the condenser C_1 and to release the relay so that a new charging period begins. Total amount of charge which flows in the input circuit in one cycle is

$$Q = C_1 E_c + I \Delta t$$

where I is the input current and

$$E_c = E - I_R$$

(R is the compensation resister R_3 + R_4 + R_5)

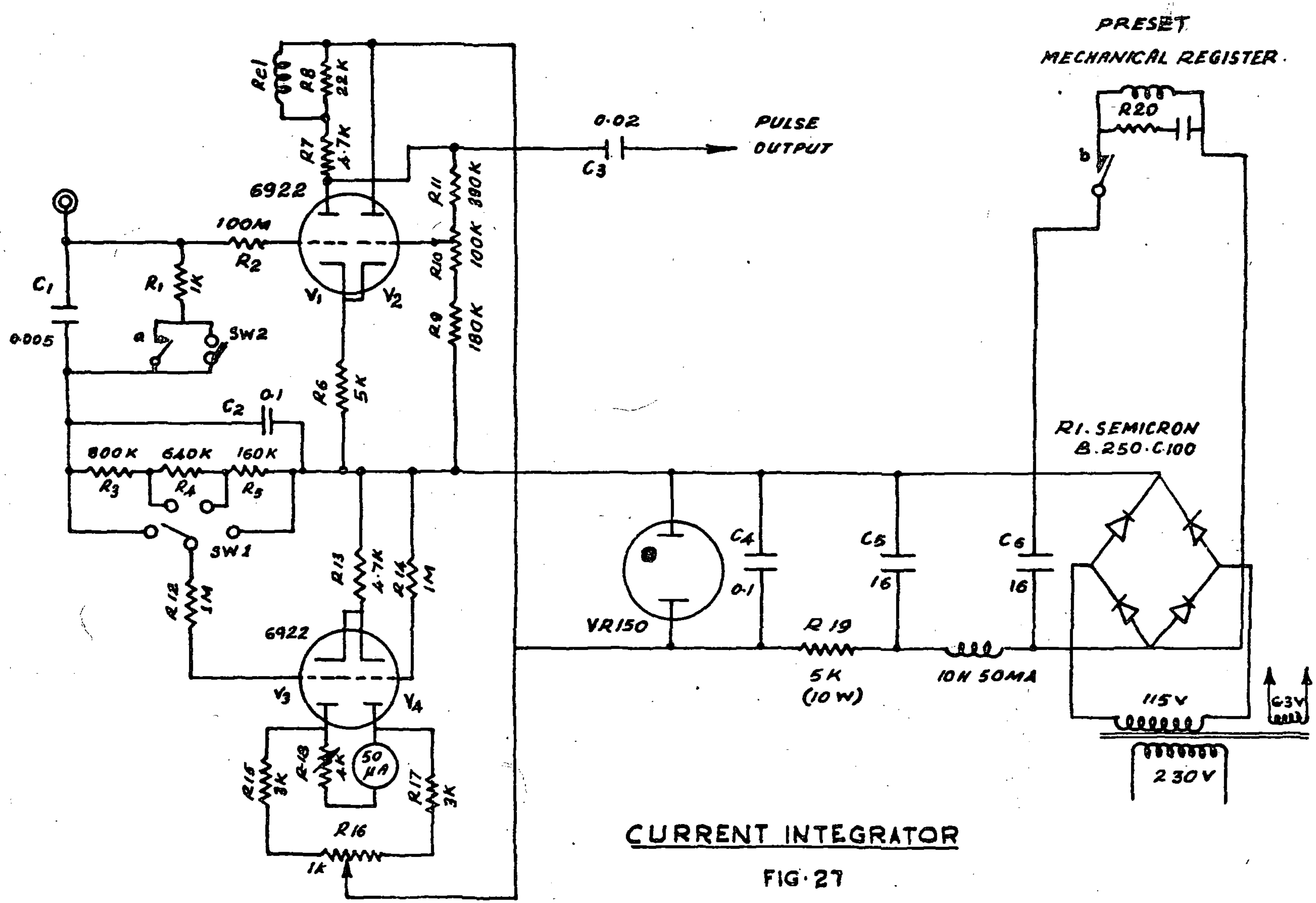

CURRENT INTEGRATOR

FIG. 27

i.e. $Q = C_1 E + I(\Delta t - R E_1)$

The equation is independent of I when $R = \frac{\Delta t}{C_1}$

With the relay used (Seimens Relay type TRLS 154 d), Δt measured is 8 ms. and with $C_1 = .005$ u F

$$R = \frac{8 \times 10^{-3}}{5 \times 10^{-9}} = 1.6 \text{ M}\Omega$$

It has been found that the integrator is linear for currents as low as 0.006 u A. Maximum input current limit is set by the mechanical register, which can handle upto 10 counts per sec. With $C_1 = .005$ u F, it can hahdle upto 1.75 u A. If it is desired to handle more current than this value, C_1 can be increased. With $C_1 = .02$ u F, the maximum input can be 7 u A. Changes in tube characteristics do not appreciably affect the calibration.

The figure for the lowest current that can be integrated is set by the testing procedure rather than the leakage current in the integrator. A reliable measurement of the low currents is therefore required.

References:

1) H.A. Enge, Rev. Sc. Instr. 23, 11 (1952) 599.

RADIATION SURVEY

G.Muthukrishnan *

During the period under the report deuteron beam was used for experiments in the Van de Graaff Accelerator. In order to assess the neutron radiation levels at various places in the beam room, survey was conducted at various operating potentials of the accelerator. The fast neutron counter[1)] developed by the R.H.C. Section was used for survey purposes. It was calibrated with the standard 50 mc Ra-Be source and its sensitivity was found to be 34 CPM/MpL.

The results of the fast neutron survey conducted at various places in the beam room with deuteron beam, at various energies, hitting the stopper and the target are tabulated below:

Deuteron Energy MeV	Beam current uA	Bombarded material	Location	Neutron level MPL	Flux Neutrons cm^2/sec.
2	1.7	Tantalum stopper	3 meters from the analysing magnet	0.4	8
2	1.7	Tantalum stopper	Beam steerer	1.0	20
2	0.5	Mg target	Fixed monitor near the Beam Room entrance	0.7	14
3.5	0.5	Tantalum stopper	Stopper	340.5	6810
4.0	0.5	Tantalum stopper	3 meters from the stopper in backward direction	2.2	44
4.5	0.5	Tantalum stopper	3 meters from the stopper in backward direction	3.0	60

* Health Physics Division

Neutrons are assumed to have energy greater than 1.0 MeV. One MPL corresponds to a flux of 20 neutrons/cm^2/sec. in the energy range of 1.0 to 10 MeV.

An analysis of the results show that in general the fast neutron level at various places in the beam room was greater than one MPL. The neutron level was found to be increasing with the focus pick-up. For example, with 0.5 uA deuteron beam at 2.0 MeV energy (Focus pick-up 1.5 uA), the fast neutron field near the fixed monitor was found to be 0.7 MPL. Under identical conditions, with 4.0 uA focus pick-up, the fast neutron field at the same place was found to be 1.7 MPLs.

Reference:

1) K.B.S. Murthy et al. "A counter for fast neutron Dosimetry" Report - AEET/H.P./D-1.

SEMINARS

Weekly seminars have become part of the activities in the laboratory. A series of six stimulating lectures on "Nilsson's model and its application" were given by Dr. K.H.Bhatt of the Physical Research Laboratory, Ahmedabad. Shri B.V.Joshi gave a course of lectures on "Transistors - Theory and practice".

WORKSHOP

The Nuclear Physics Division workshop in this laboratory has fabricated a number of components required for the operation and maintenance of the accelerator and auxiliary equipment and also catered for all the requirements of the accelerator development group and the various research groups working with the accelerator. Some of the equipment fabricated during the period under report are: Thermo-mechanical leak systems, liquid nitrogen traps, high voltage bushings, quadrupole focusing lens assembly, beam steerer assembly, corona collector units, target chamber for charged particle experiments and table with two plane movements for angular correlation experiments. Design drawings for the new 5-port beam switching magnet has been completed and the aluminium switching chamber is under fabrication.

The workshop has also fabricated for the scientists of Nuclear Physics Division working at CIRUS, APSARA and ZERLINA - a number of equipments such as gas flow cryostat, analysing spectrometer, polarised neutron spectrometer, a cam driven set up for the study of Mossbauer effect, thermalising tank assembly and also various component for fission experiments and neutron time of flight experiments.

INDIAN NUCLEAR DATA GROUP

C. Badrinathan*, M. Balakrishnan, H.G. Devare*
A.S.Divatia, D.N. Kundu**, B.P.Rastogi
M.Srinivasan and G. Venkataraman

The major activity of the Indian Nuclear Data Group (INDG) has been compilation of reports. Information relevant to Nuclear Data collected from various laboratories is compiled into reports for submission to International Nuclear Data Scientific Working Group (INDSWG) of the International Atomic Energy Agency.

The INDG is now a full fledged contributor to the CINDA (Computor Index Neutron Data) programme of the INDSWG. All relevant Indian Journals and reports are scanned regularly from nuclear data and the information is sent to the INDSWG.

A programme for measuring (α, n) and (p, n) cross sections has been started. Useful (n, α) and (n, p) cross sections can be obtained using reciprocity $^{16}O(n, \alpha)^{13}C$ cross sections have been obtained in this way (see page 23 of this report).

Resonance absorption and resonance scattering studies are being carried out. Programmes for the calculation of resonance integrals, written for the IBM-7090 computor have been adapted for use on the CDC-3600 computor. Programme for optical model calculations and for obtaining resonance scattering cross sections are also being adapted for the CDC-3600 computor.

All reports pertaining to Nuclear Data are maintained separately in the Physics Group Library at Van de Graaff Laboratory

---

* Tata Institute of Fundamental Research, Bombay.
** Saha Institute of Nuclear Physics, Calcutta.

LIBRARY

The Physics Group Library at Van de Graaff grew to fill the space allotted to it. Additional space was given to the Library in July 1965. The library was then reorganised with addtion of more racks to facilitate 'open access'.

Library collection: 638 books and 244 Bound Volumes of periodicals were received during the year. This represents an increase of 25% over the previous years total number of volumes in the library. On December 31,1965 the library had 2742 books and 1606 bound volumes of periodicals (4348 volumes in all - as compared to 3466 in 1964).

In addition there is an increase in receipt of AEET reports and reprints

Catalogue: A complete classified catalogue based on Universal Decimal Classification has been made available to the readers, which was under preparation last year.

Periodicals: One more journal 'Nuclear Physics' was being obtained by Air Mail during the year bringing the total number of periodicals so obtained in the library to six. There is a general increase in the receipt of new journals subscribed during the year bringing the total number to about 100 titles.